

Ionic liquid gating of $\text{YBa}_2\text{Cu}_3\text{O}_{7-x}$ grain boundaries

A. Fête, C. Senatore

3MO3 - Cuprate Thin films

Brief introduction to grain boundaries in YBCO and ionic liquid gating

Brief introduction to grain boundaries in YBCO and ionic liquid gating

Device structure and efficiency

Brief introduction to grain boundaries in YBCO and ionic liquid gating

Device structure and efficiency

Results obtained on a 8° boundary

Brief introduction to grain boundaries in YBCO and ionic liquid gating

Device structure and efficiency

Results obtained on a 8° boundary

Summary of the results obtained on 2° - 3° - 5° boundaries

Brief introduction to grain boundaries in YBCO and ionic liquid gating

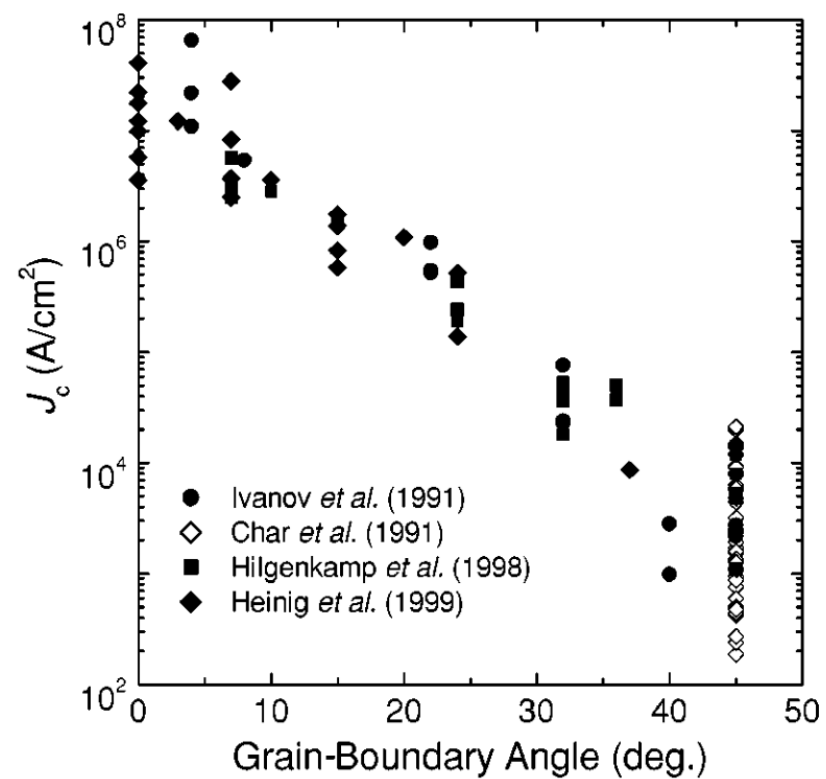
Device structure and efficiency

Results obtained on a 8° boundary

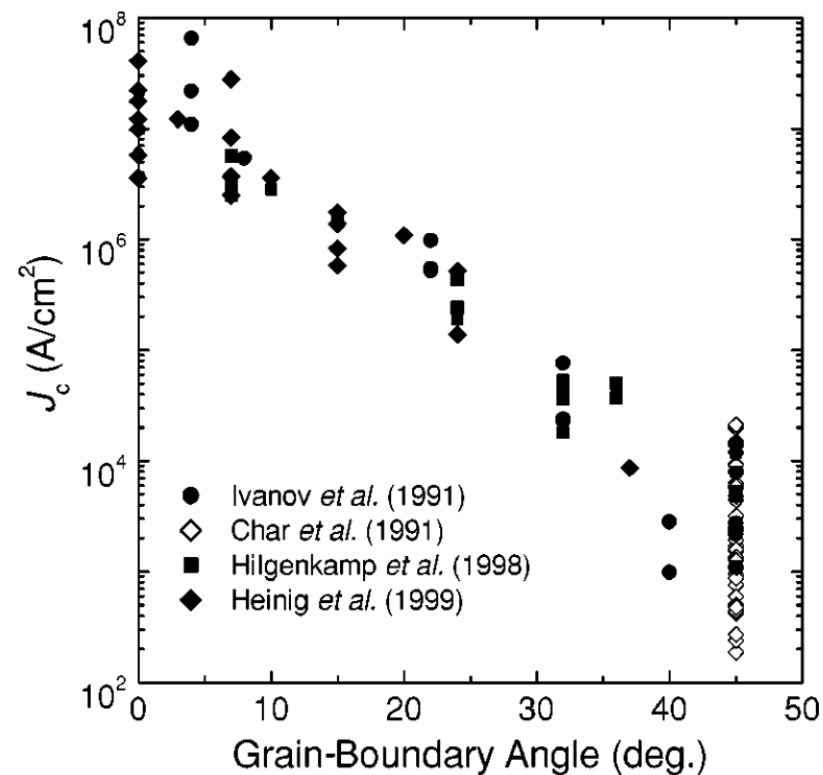
Summary of the results obtained on 2° - 3° - 5° boundaries

Conclusion and perspectives

Impact on SC transport

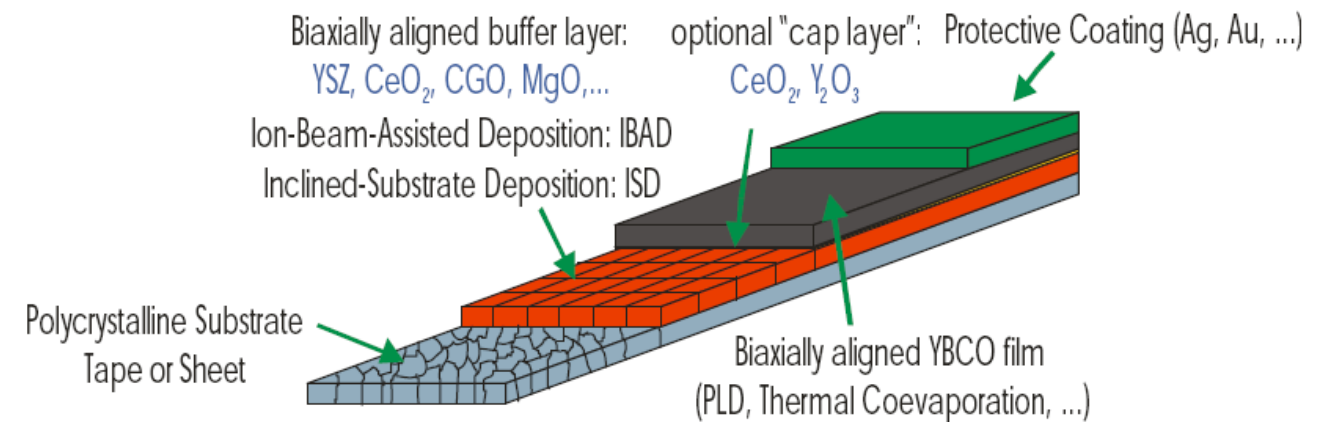


Hilgenkamp and Mannhart, RMP **74** 485 (2002)

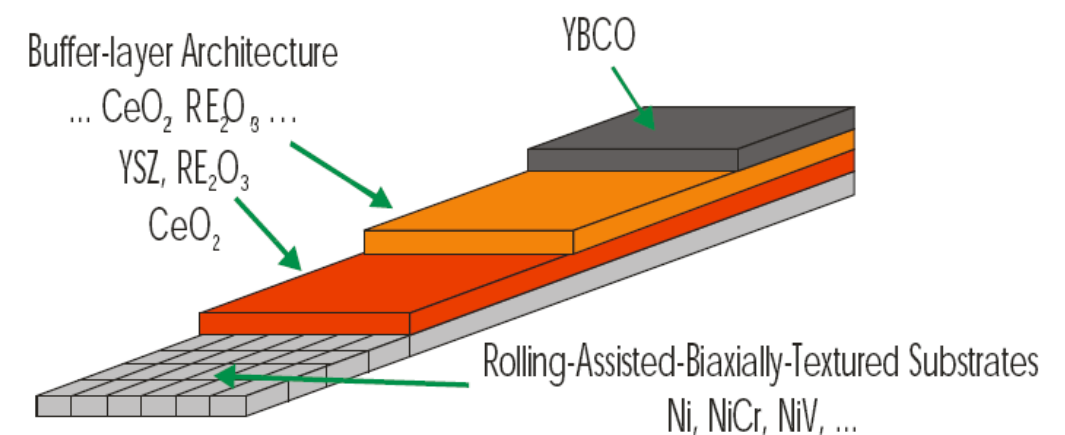


Hilgenkamp and Mannhart, RMP **74** 485 (2002)

Forced Texturing IBAD, ISD



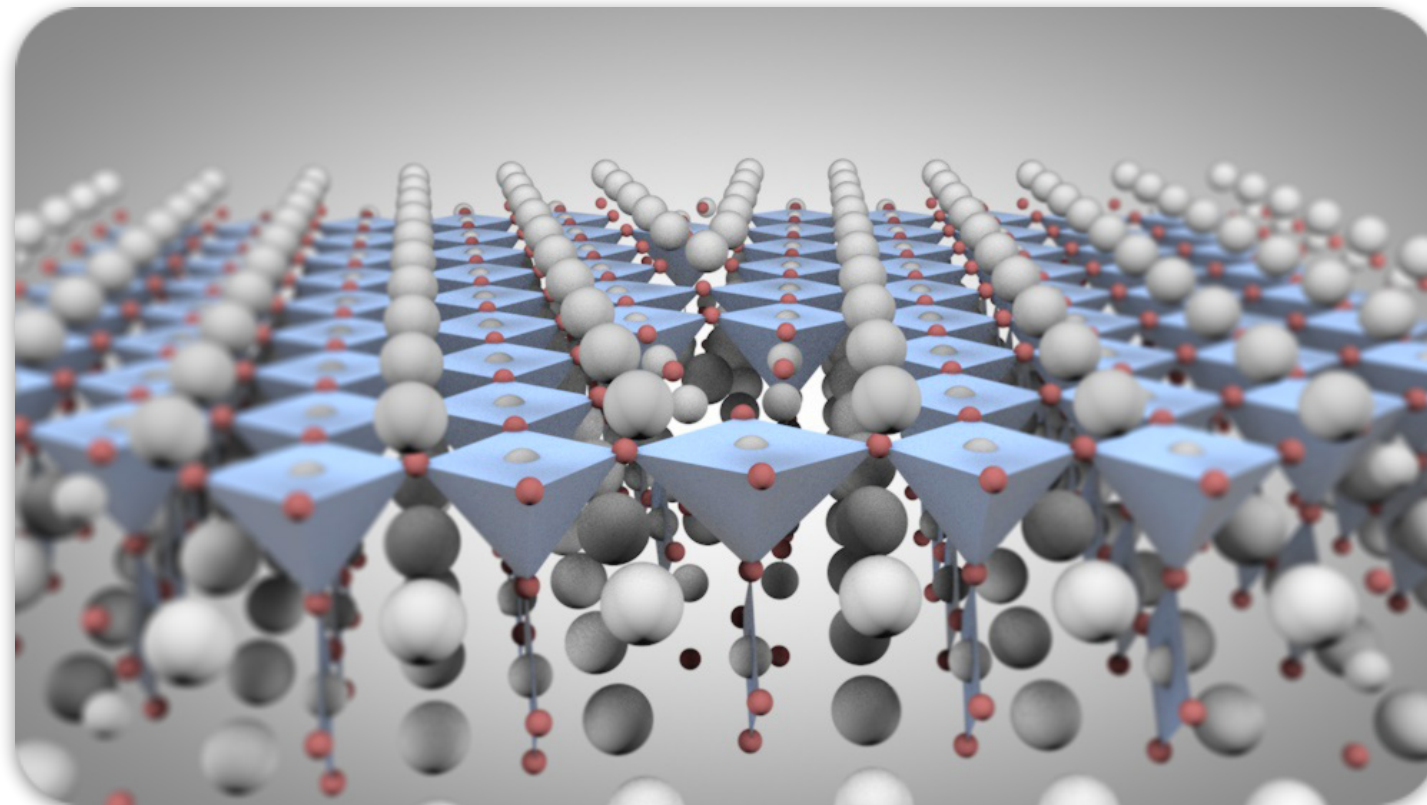
Thermo-mechanical Texturing of Substrates (TMT) RABiTS



Q: What is the dominant mechanism limiting J_c^{GB} in YBCO?

strain field

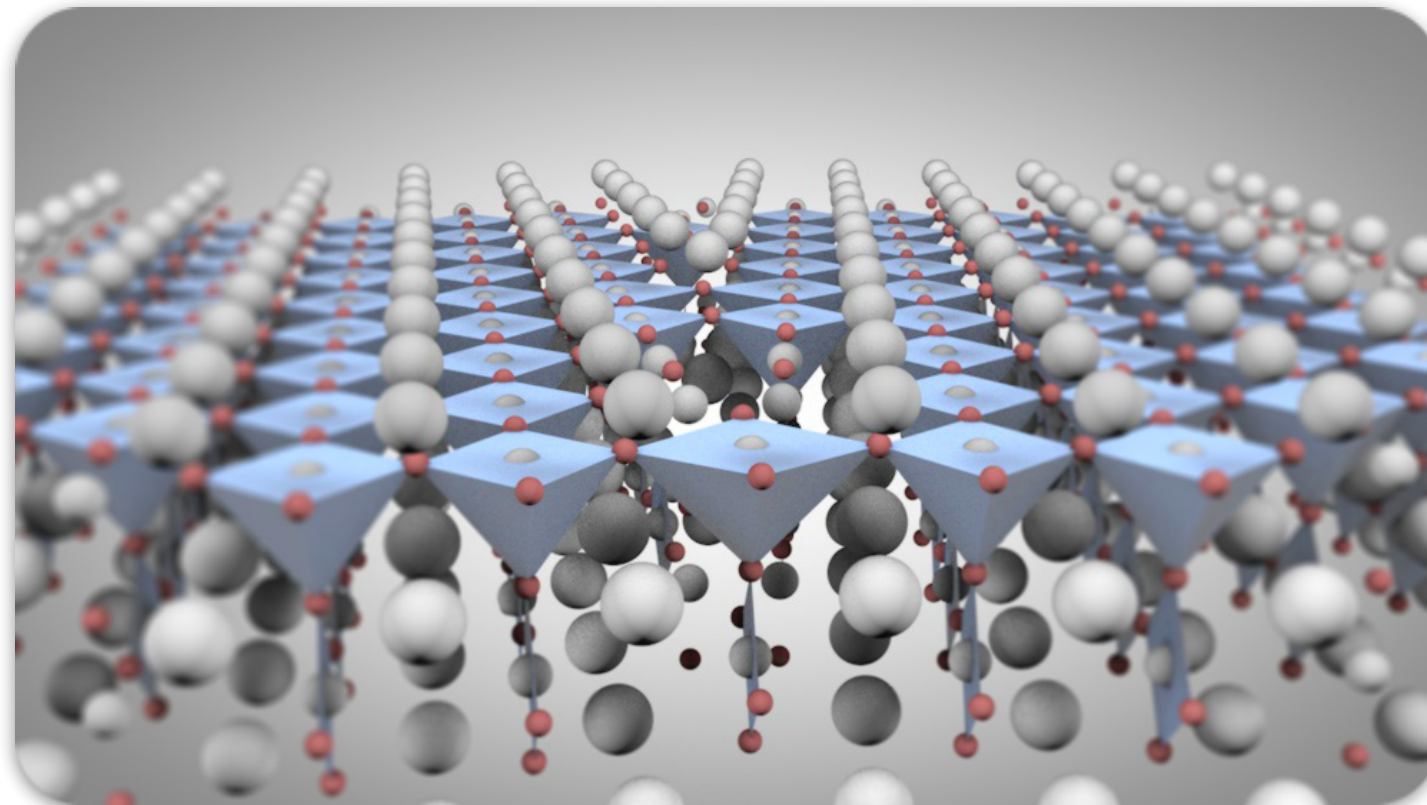
variations of the charge carrier concentration



Q: What is the dominant mechanism limiting J_c^{GB} in YBCO?

strain field

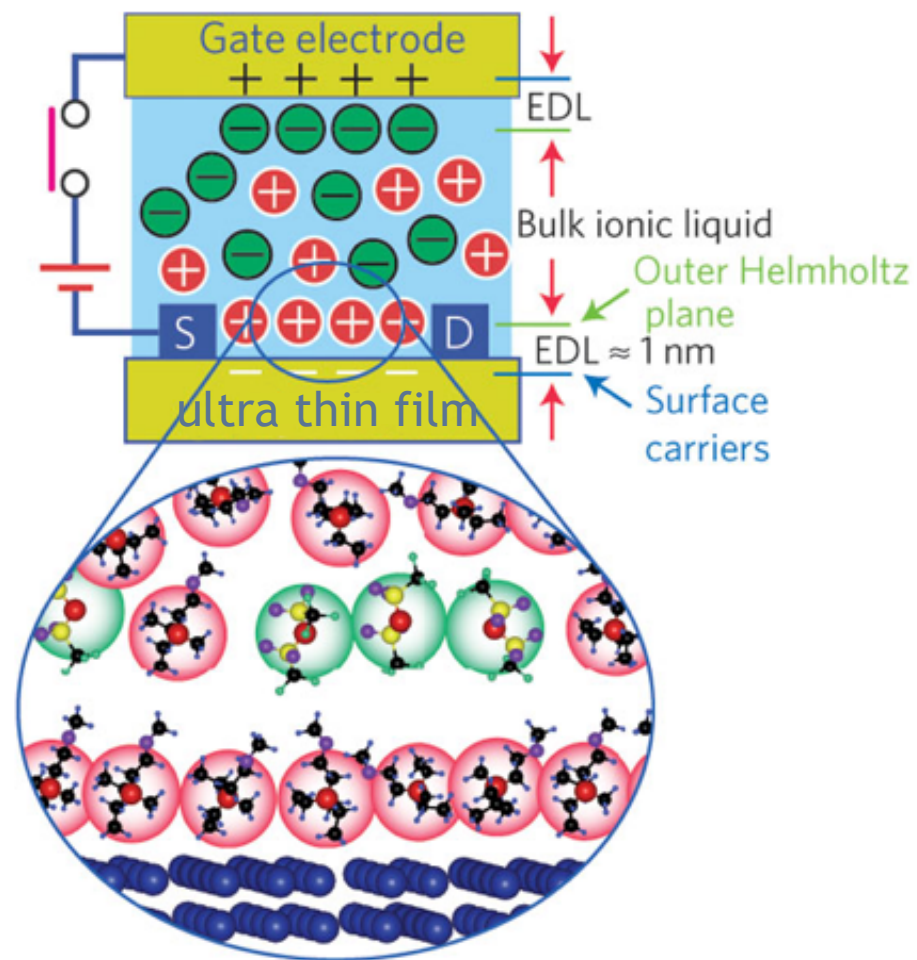
variations of the charge carrier concentration



Basics of field effect (FE)



Ionic liquid based FE device

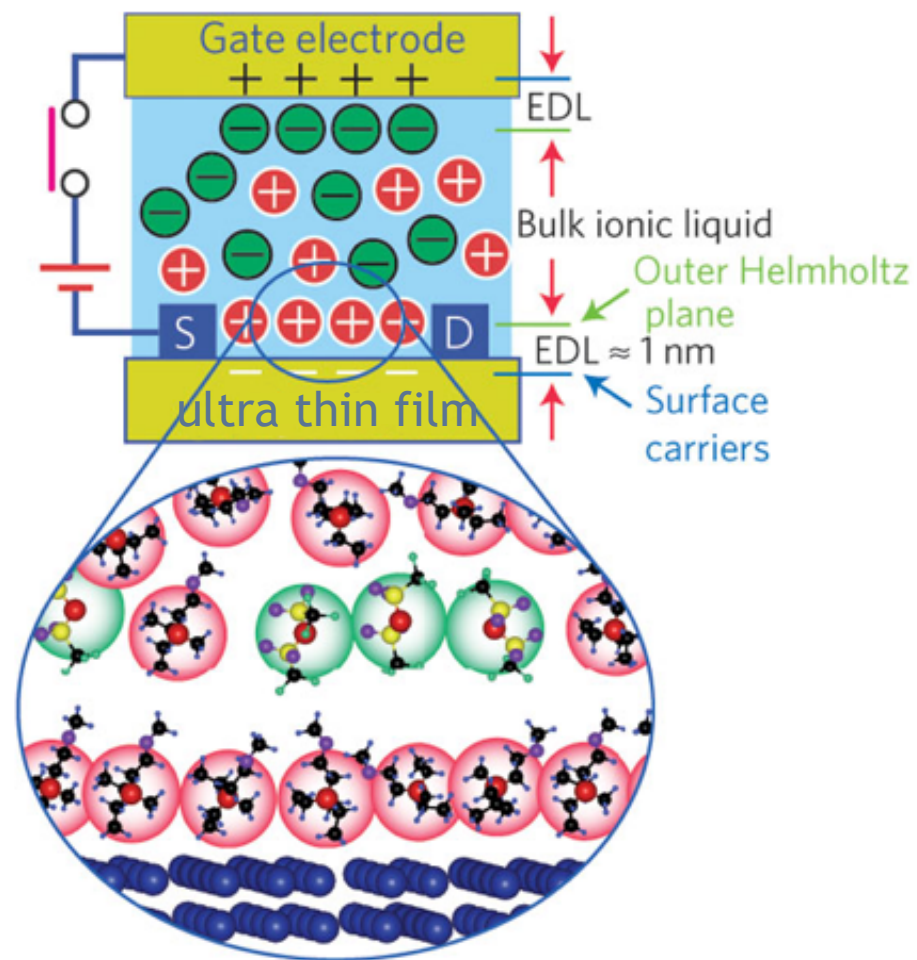


adapted from :
Ye *et al.* Nature Materials **9**, 125 (2010)

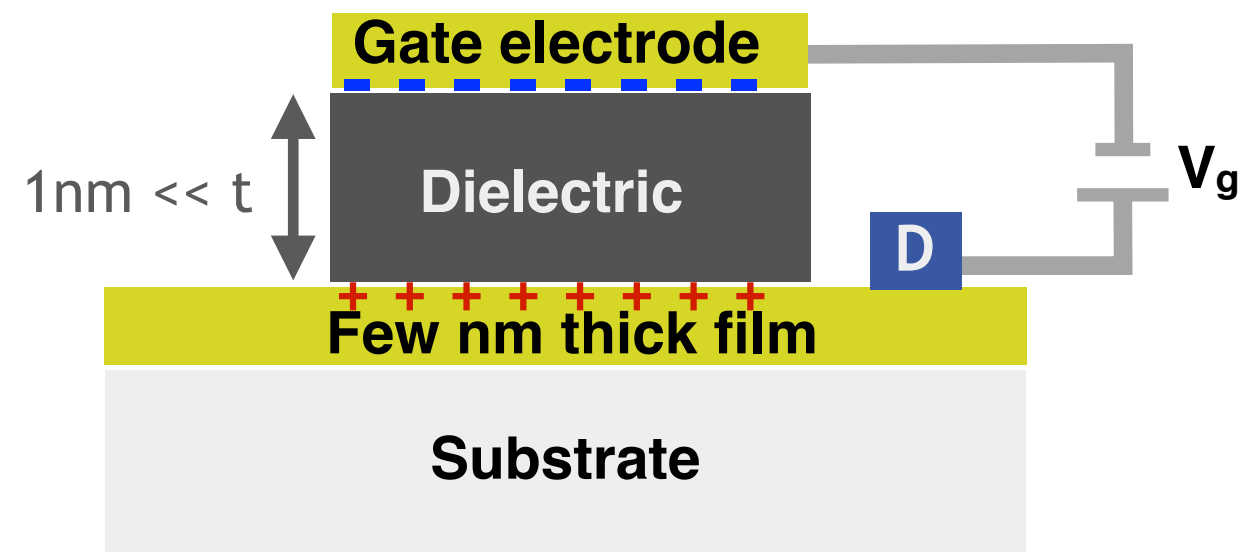
Basics of field effect (FE)



Ionic liquid based
FE device



Standard FE device
(solid dielectric)

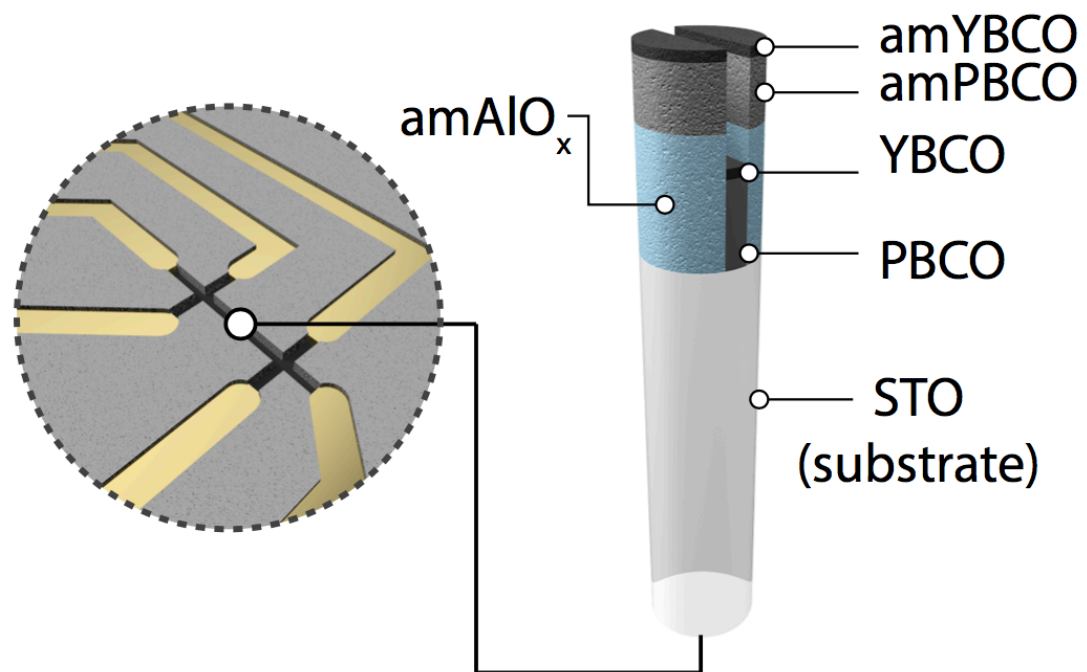
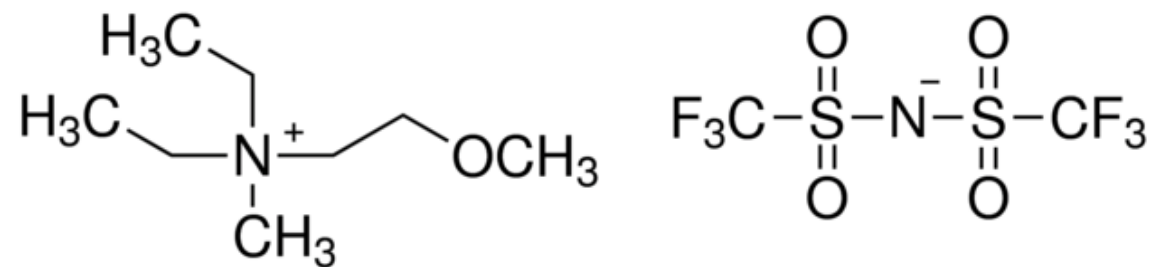


adapted from :
Ye *et al.* Nature Materials **9**, 125 (2010)

Device structure



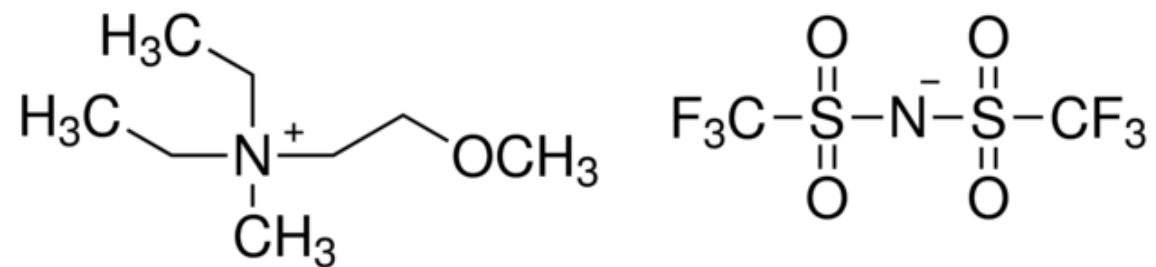
DEME⁺ - TFSI⁻



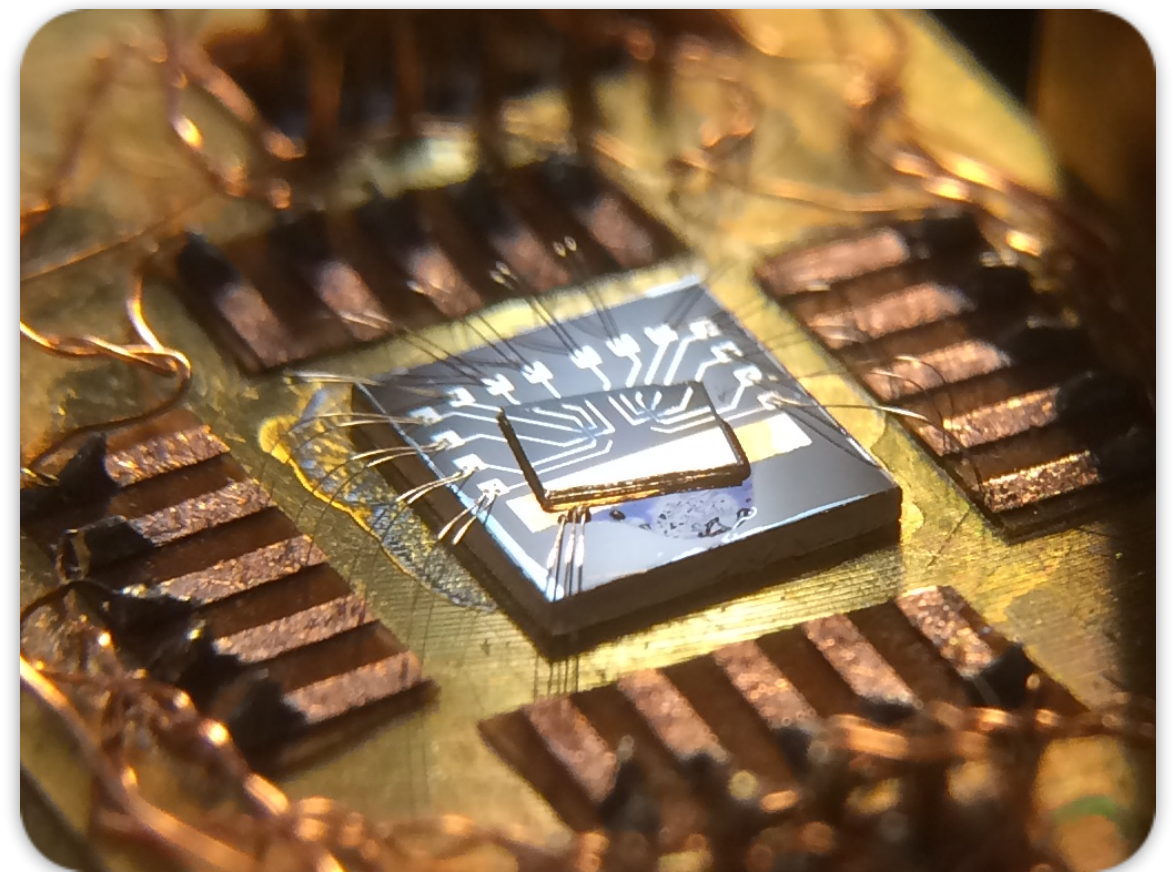
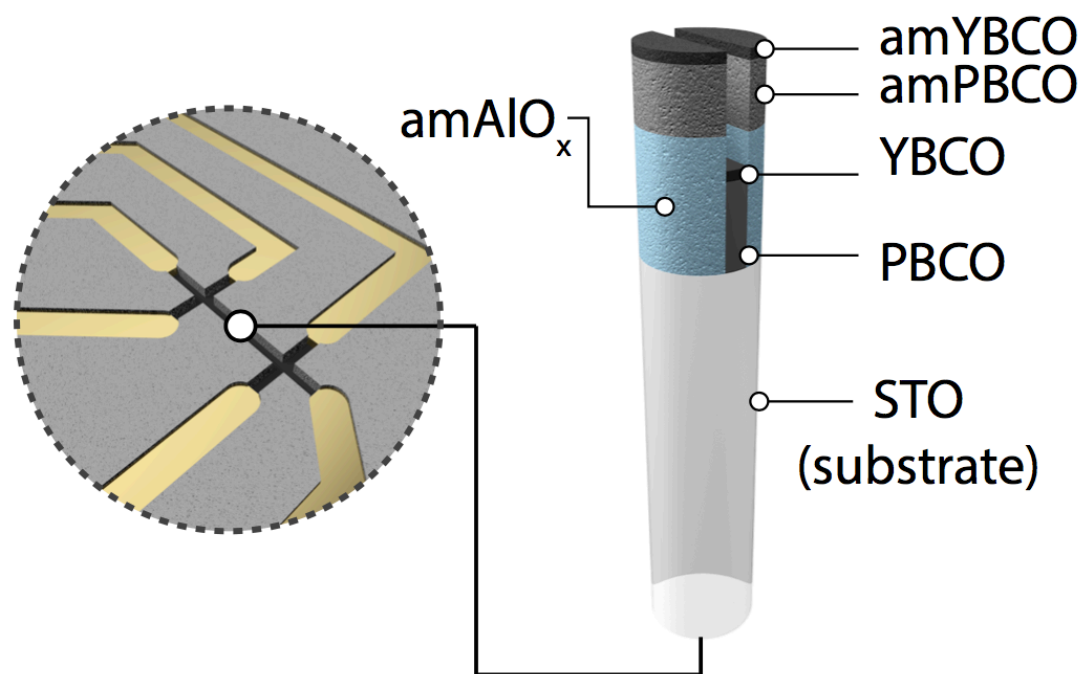
Device structure



DEME⁺ - TFSI⁻



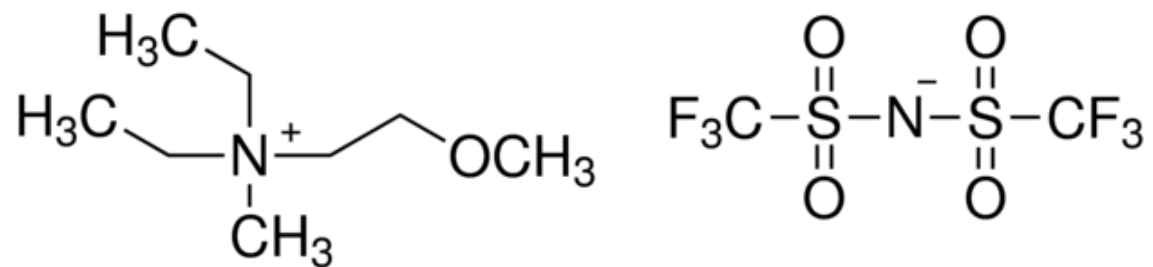
H 1 mm



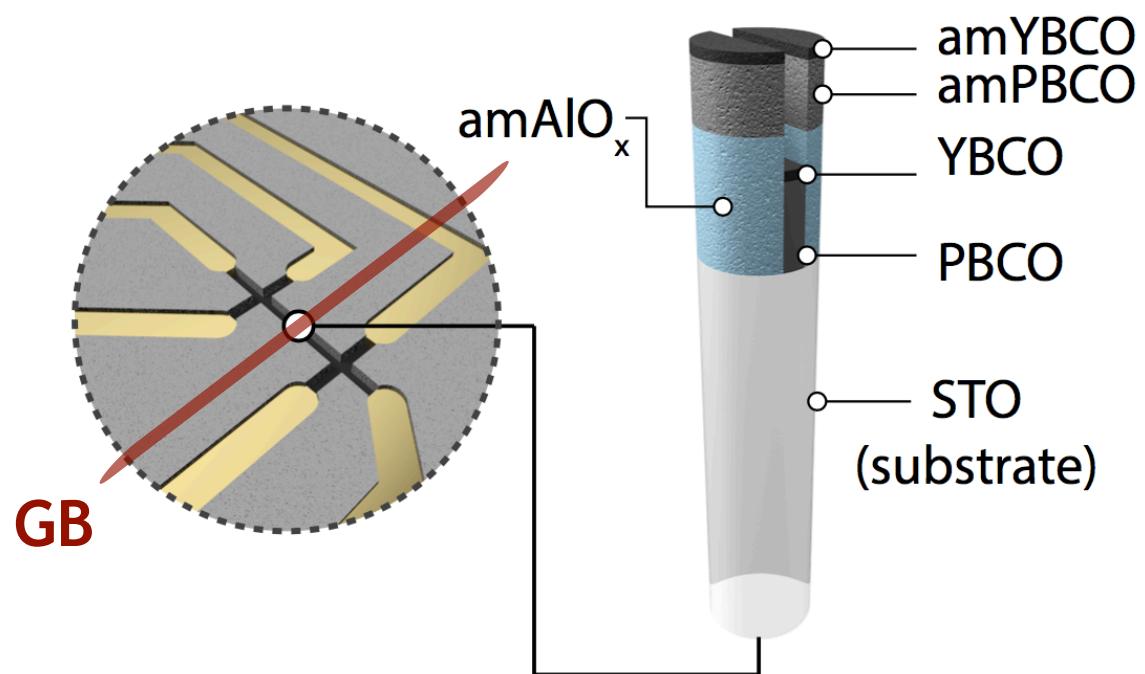
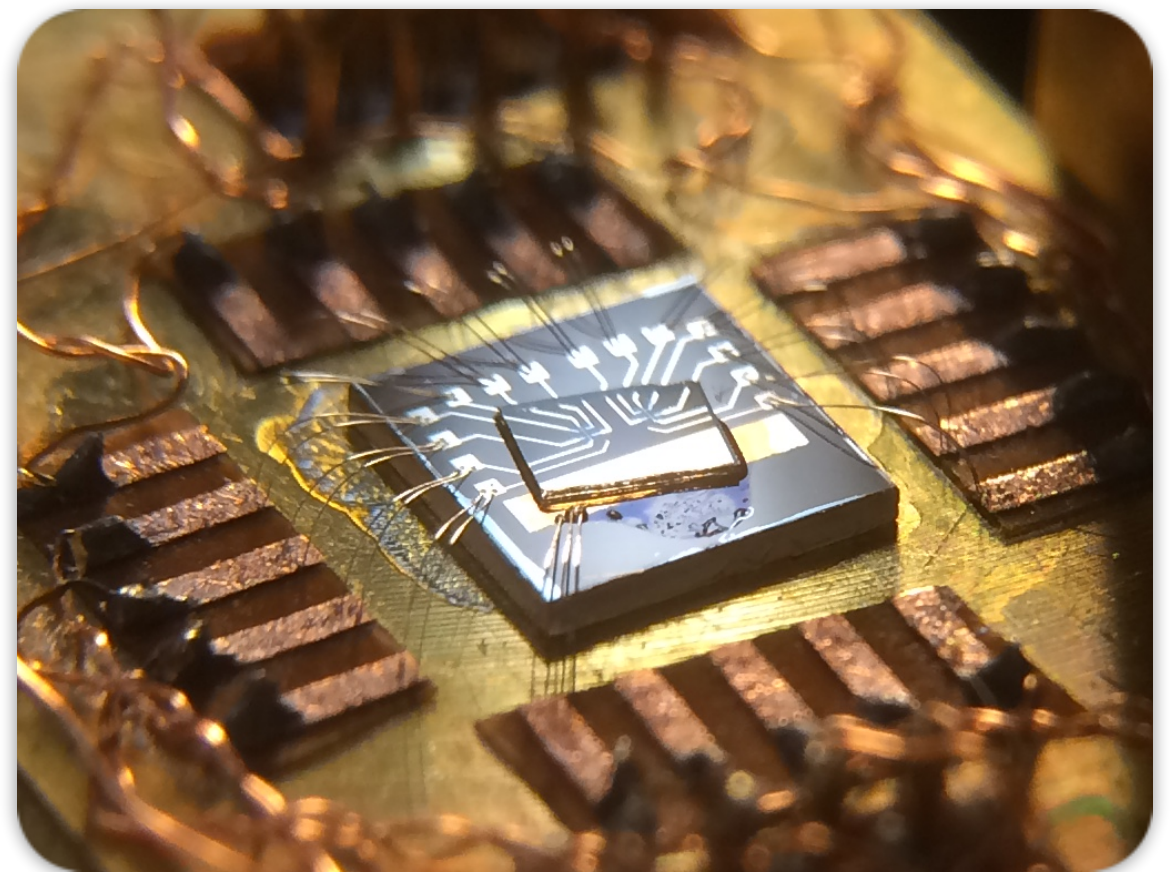
Device structure



DEME⁺ - TFSI⁻



H 1 mm



Sample preparation & characteristics



Our ultra-thin films :

on SrTiO_3 substrate ([001]-tilt
bi-crystals)

buffer layer : 20uc PBCO
SC layer : 5uc of YBCO

$T_c(R=0) \approx 60\text{K}$, capped

$T_c(R=0) \approx 45\text{K}$, uncapped and
patterned

$T_c(R=0) \approx 20\text{K}$ with ionic liquid
(device ready)

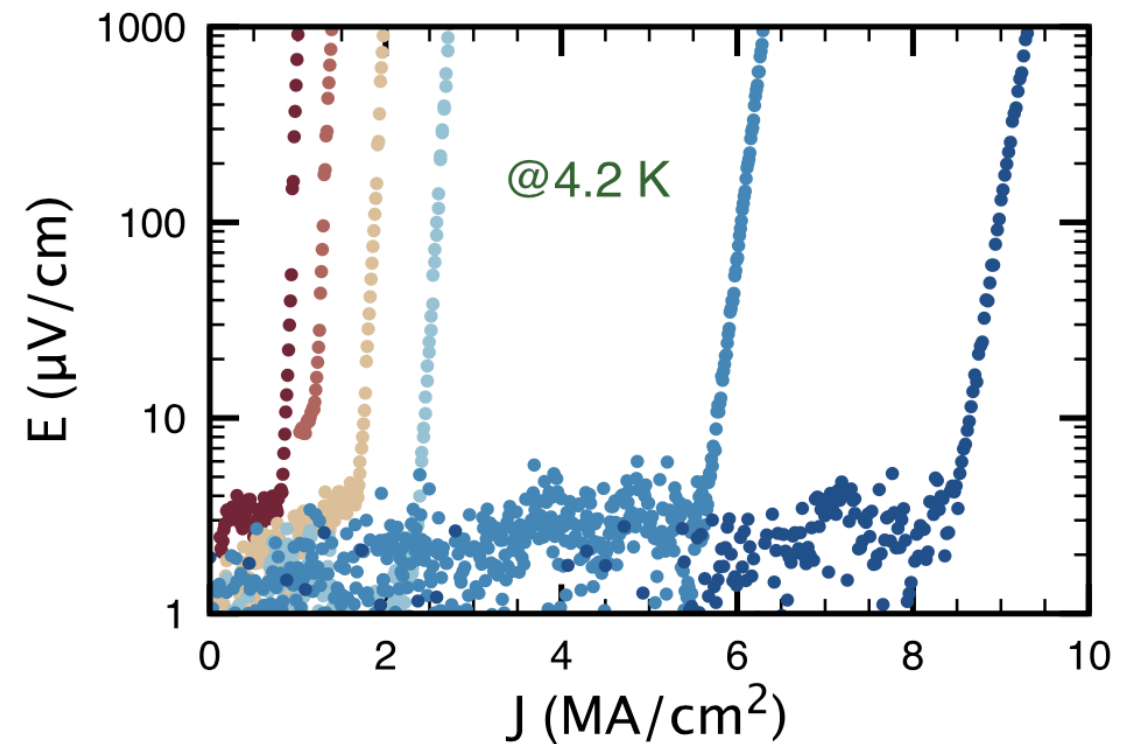
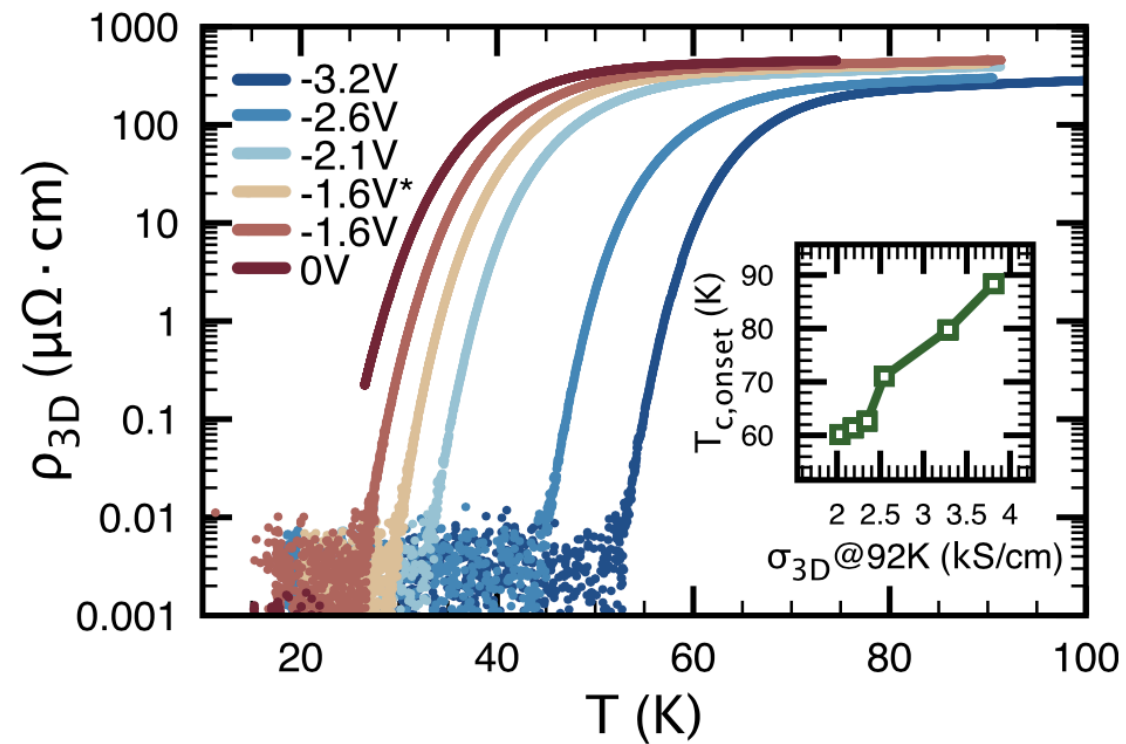
A circular inset image showing the interior of a sputtering chamber. It features a central carousel with two glowing targets (PBCO and YBCO) and a heated sample stage. The chamber is filled with an oxygen atmosphere.

**Carousel with
PBCO and
YBCO targets**

Heated sample

**O_2 atmosphere
($\approx 10^{-1}$ mbar)**

Tuning in GB free samples

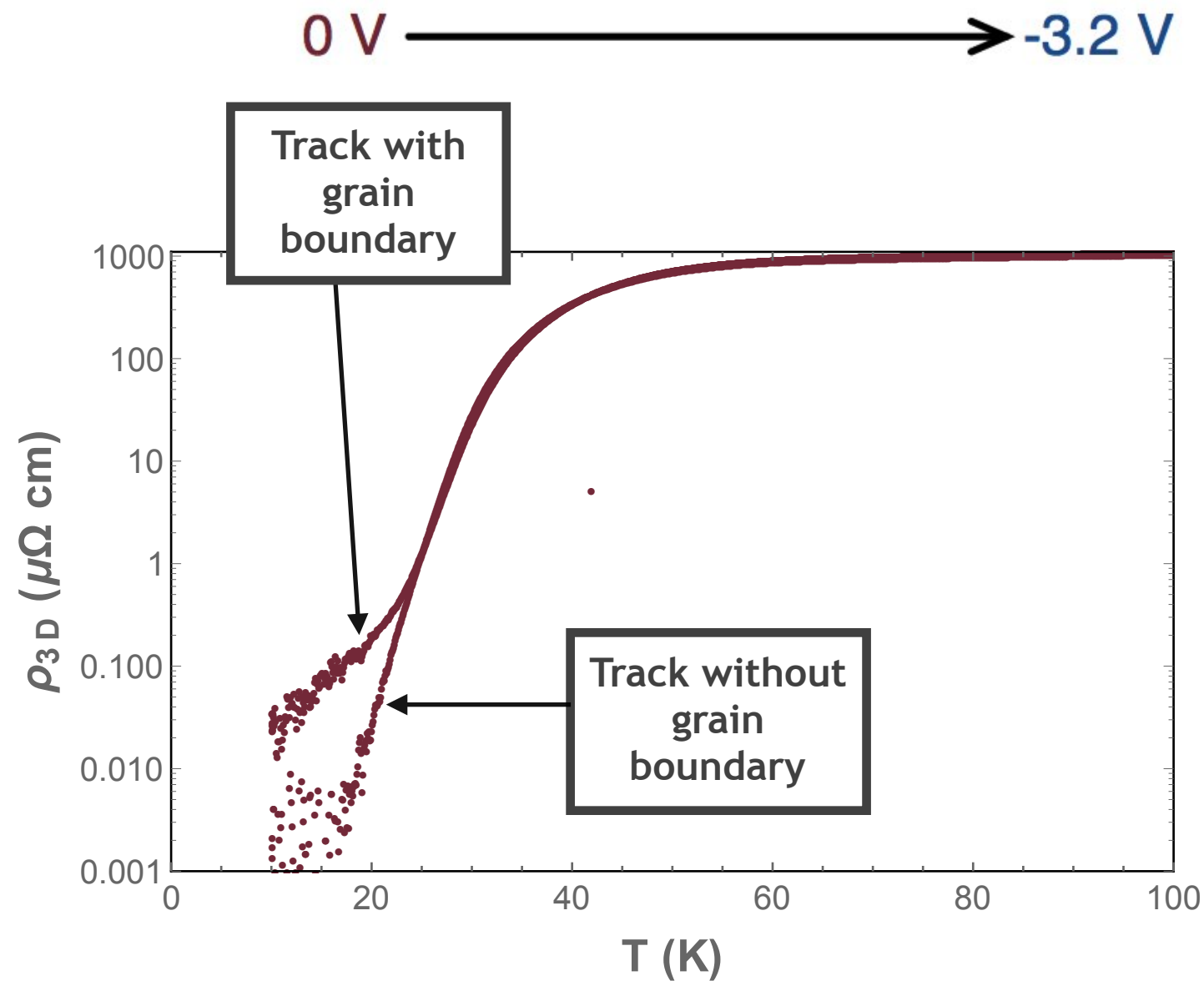


A. Fête, L. Rossi, A. Augieri, C. Senatore, APL **109** 192601 (2016)

Tuning of a [001] tilt 8° GB



Cooling in remanent field (approx. 7mT)

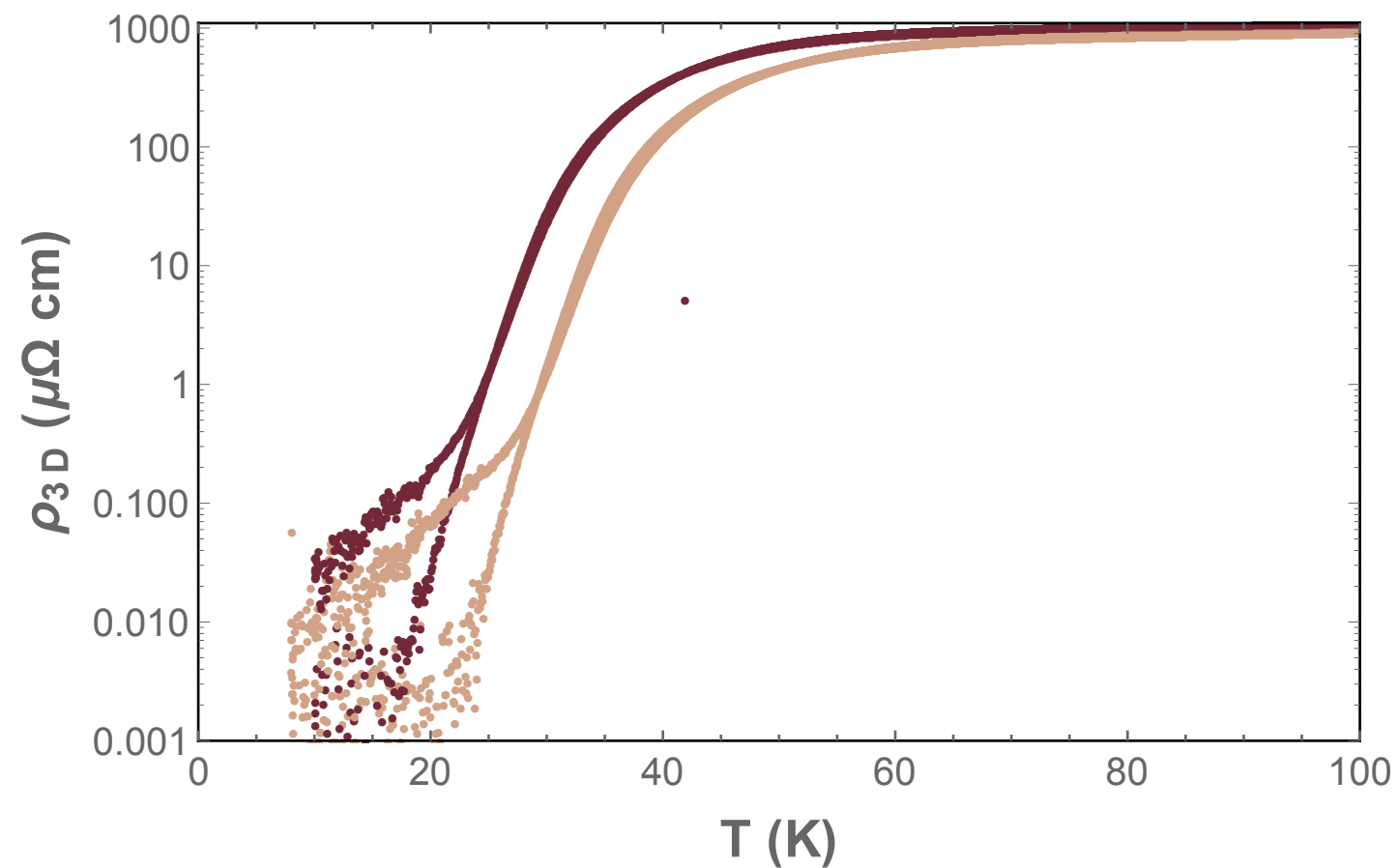


Tuning of a [001] tilt 8° GB



Cooling in remanent field (approx. 7mT)

0 V \longrightarrow -3.2 V

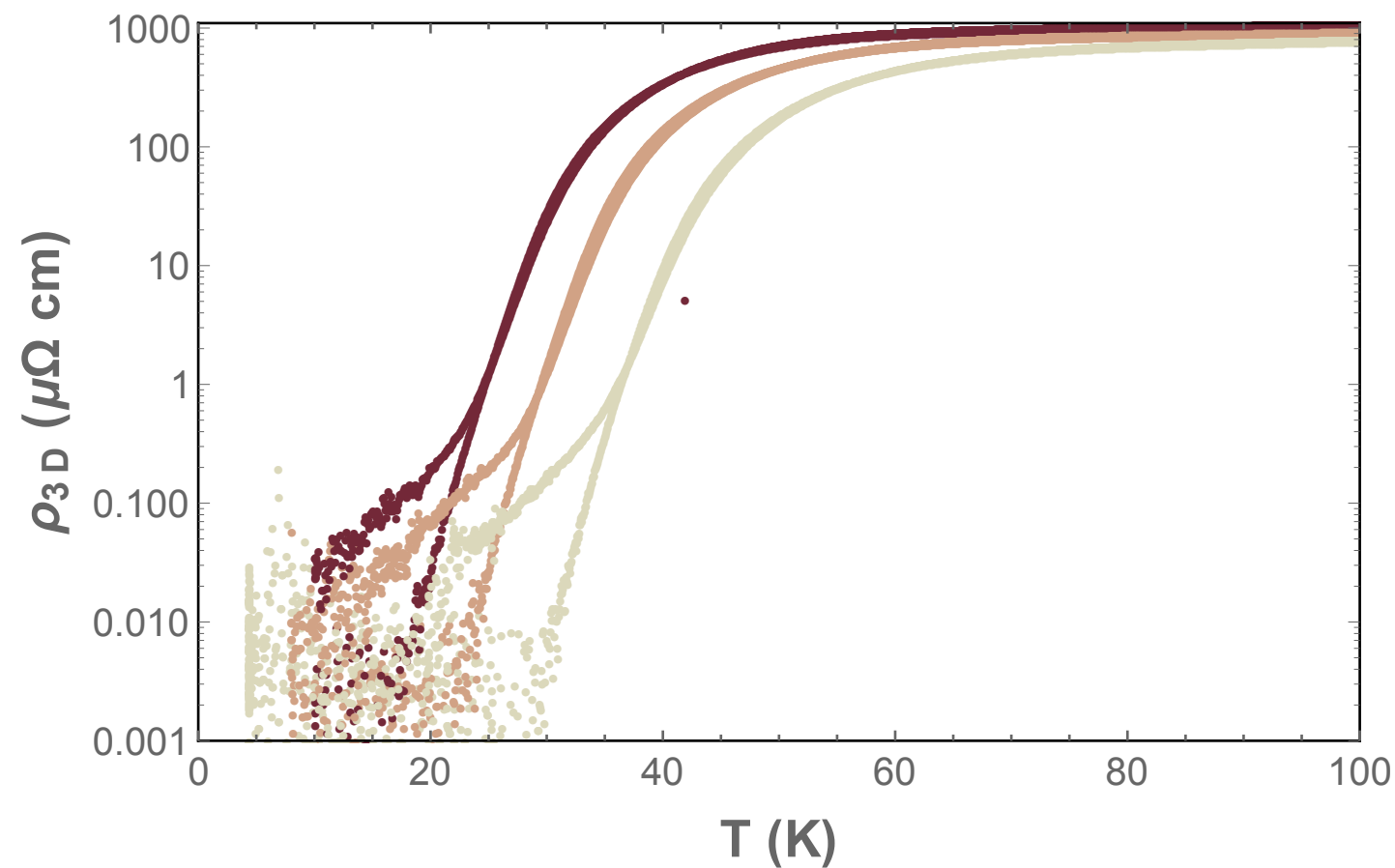


Tuning of a [001] tilt 8° GB



Cooling in remanent field (approx. 7mT)

0 V \longrightarrow -3.2 V

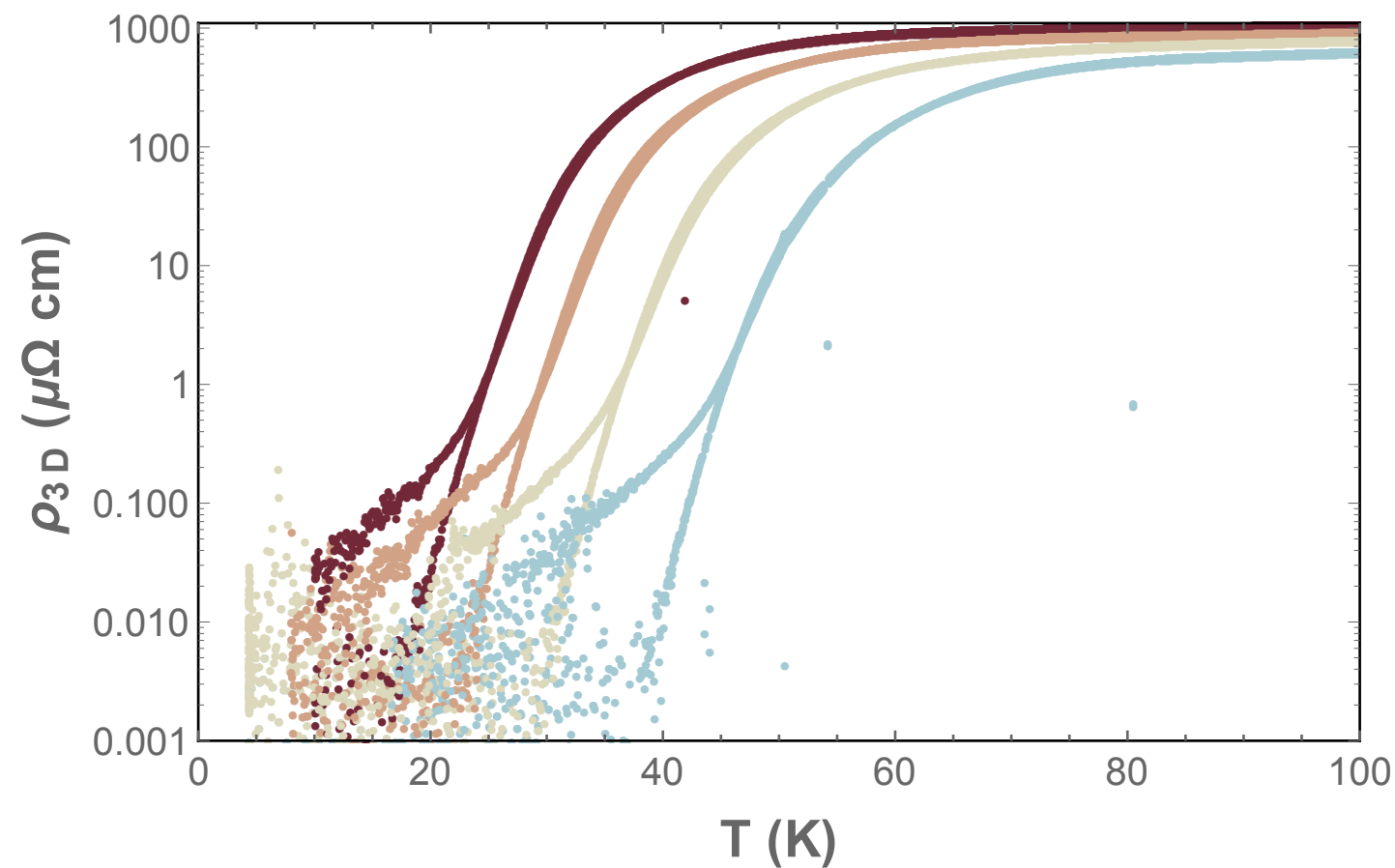


Tuning of a [001] tilt 8° GB



Cooling in remanent field (approx. 7mT)

0 V \longrightarrow -3.2 V

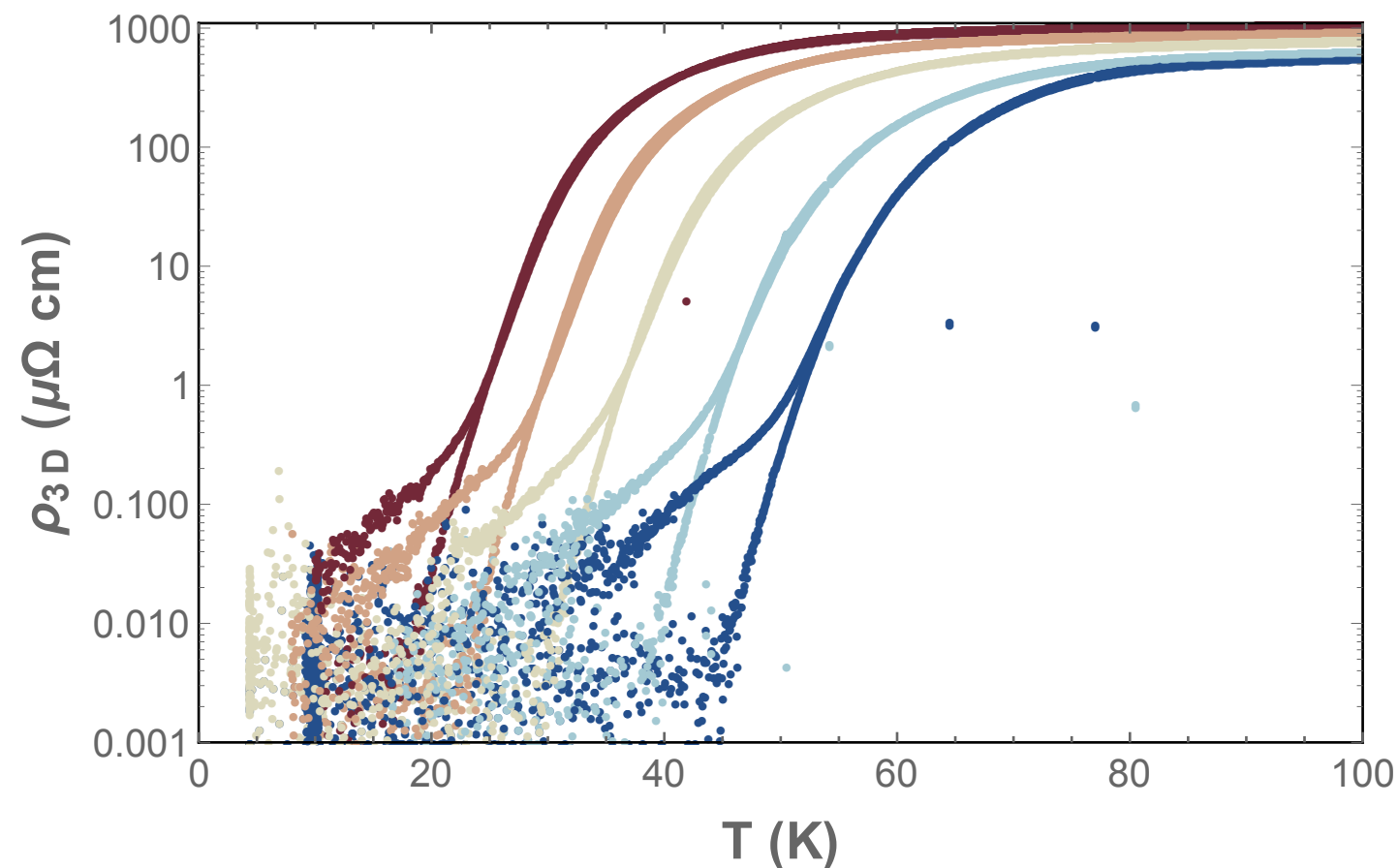


Tuning of a [001] tilt 8° GB



Cooling in remanent field (approx. 7mT)

0 V \longrightarrow -3.2 V



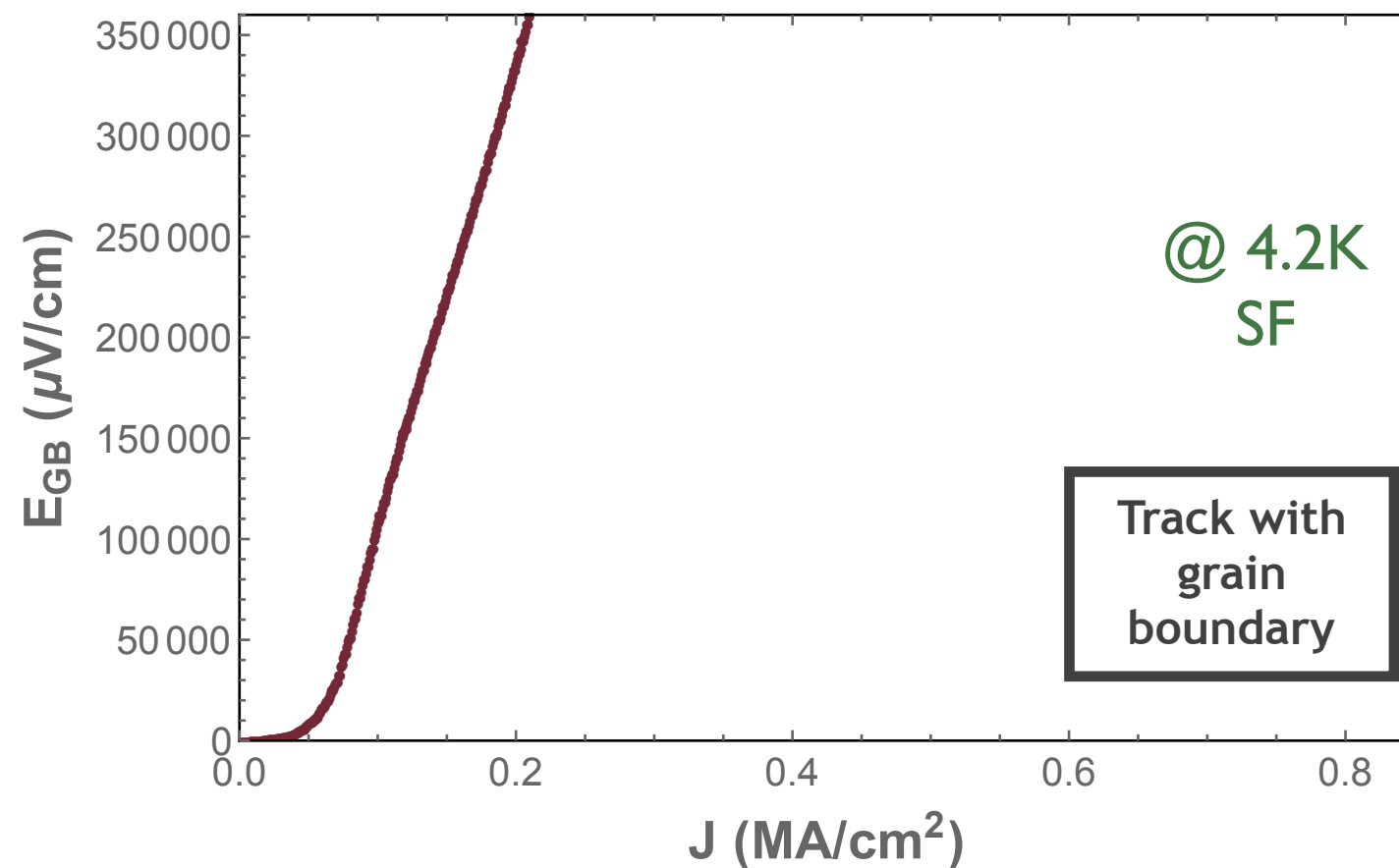
A clear increase of T_c with doping is observed on both the intra- and inter-grain channels

Tuning of a [001] tilt 8° GB



Cooling in remanent field (approx. 7mT)

0 V \longrightarrow -3.2 V

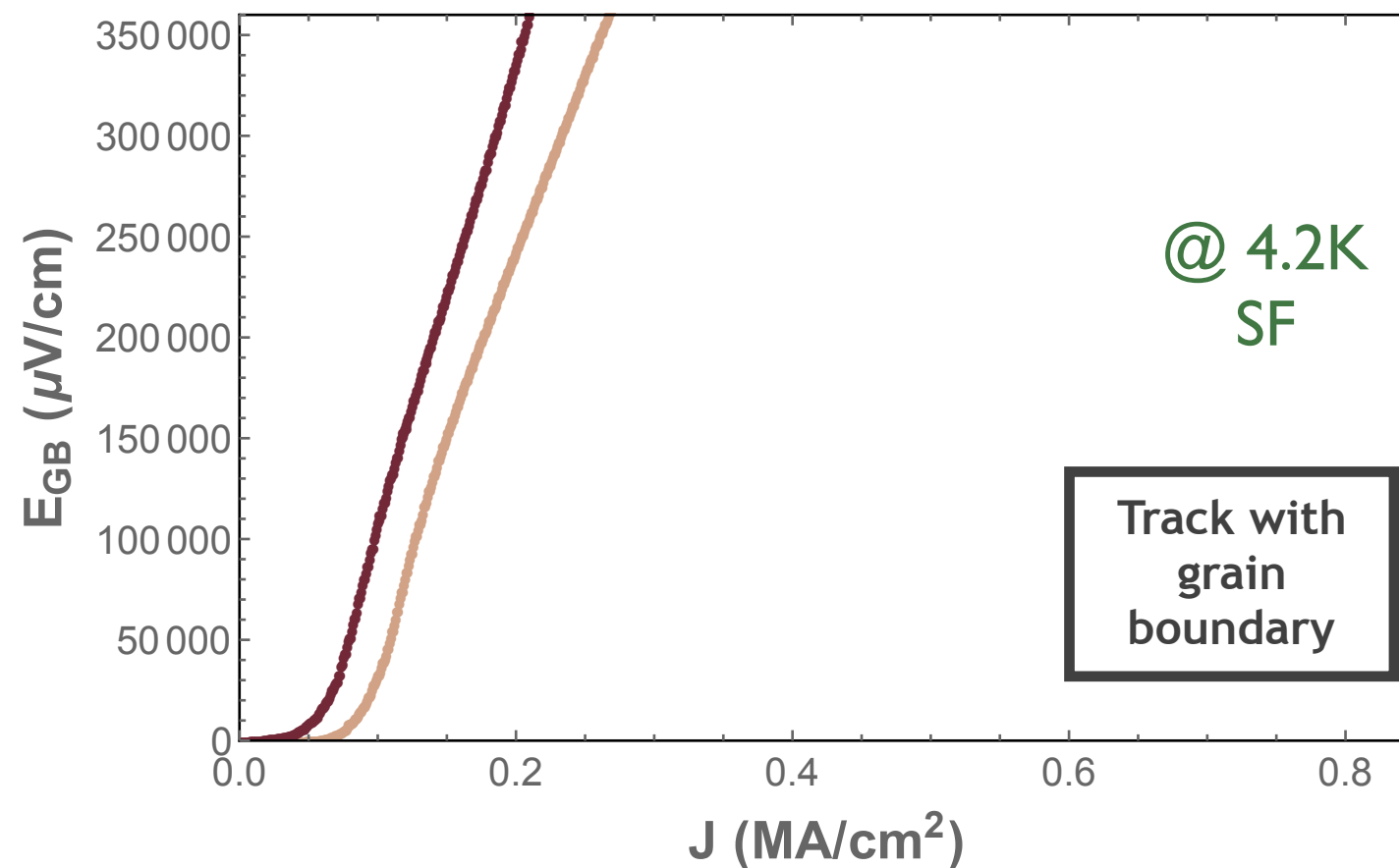


Tuning of a [001] tilt 8° GB



Cooling in remanent field (approx. 7mT)

0 V \longrightarrow -3.2 V

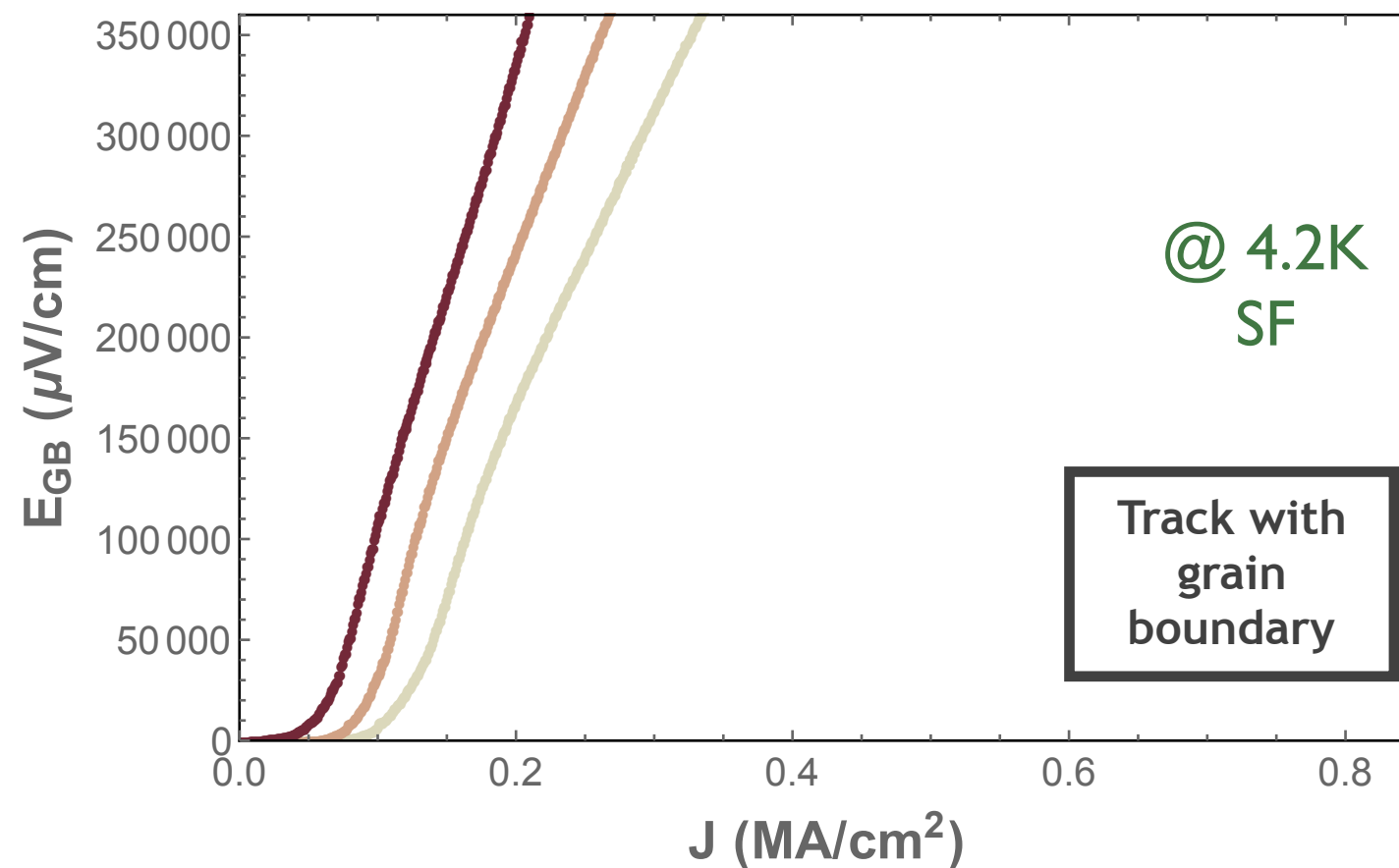


Tuning of a [001] tilt 8° GB



Cooling in remanent field (approx. 7mT)

0 V \longrightarrow -3.2 V

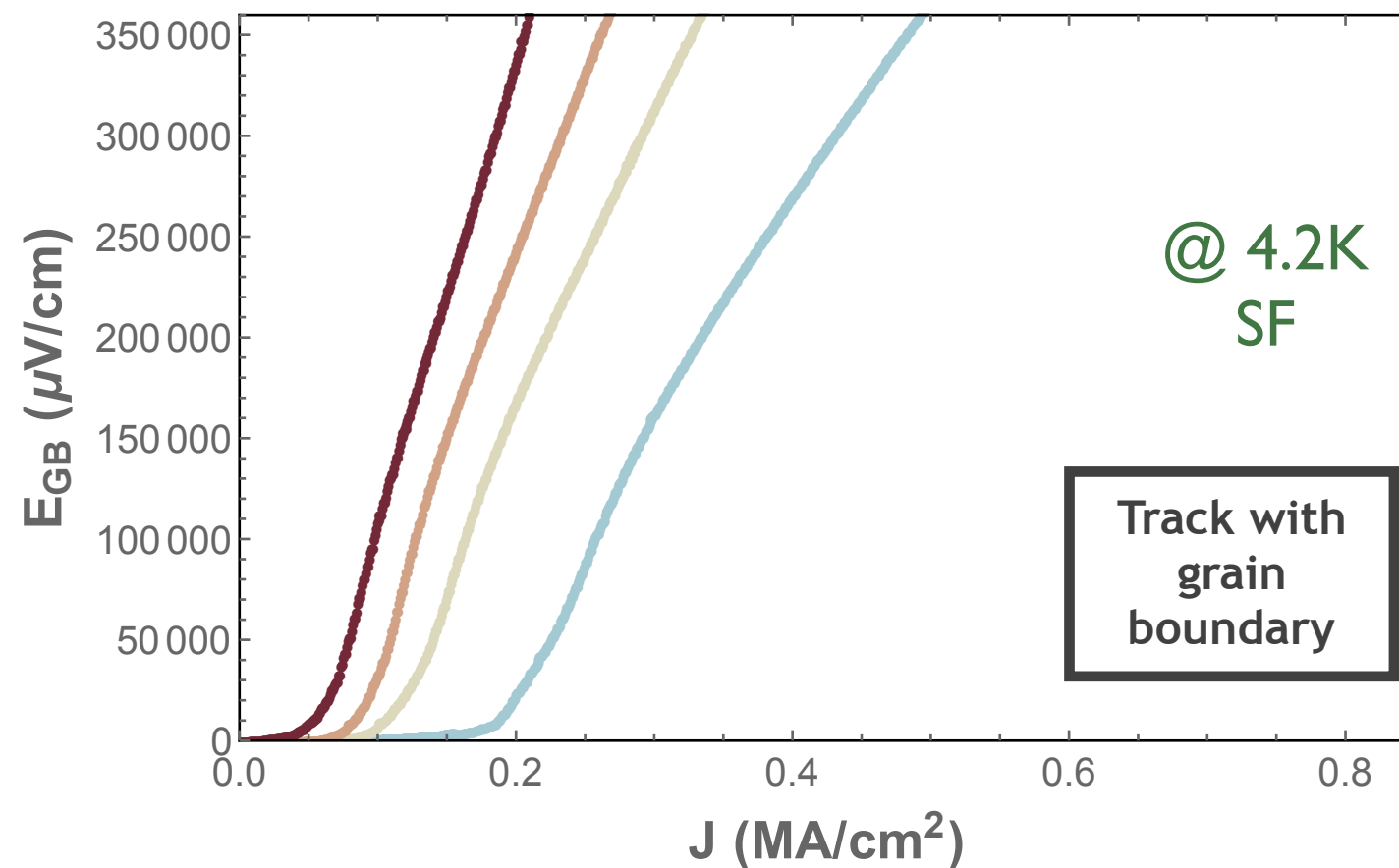


Tuning of a [001] tilt 8° GB



Cooling in remanent field (approx. 7mT)

0 V \longrightarrow -3.2 V

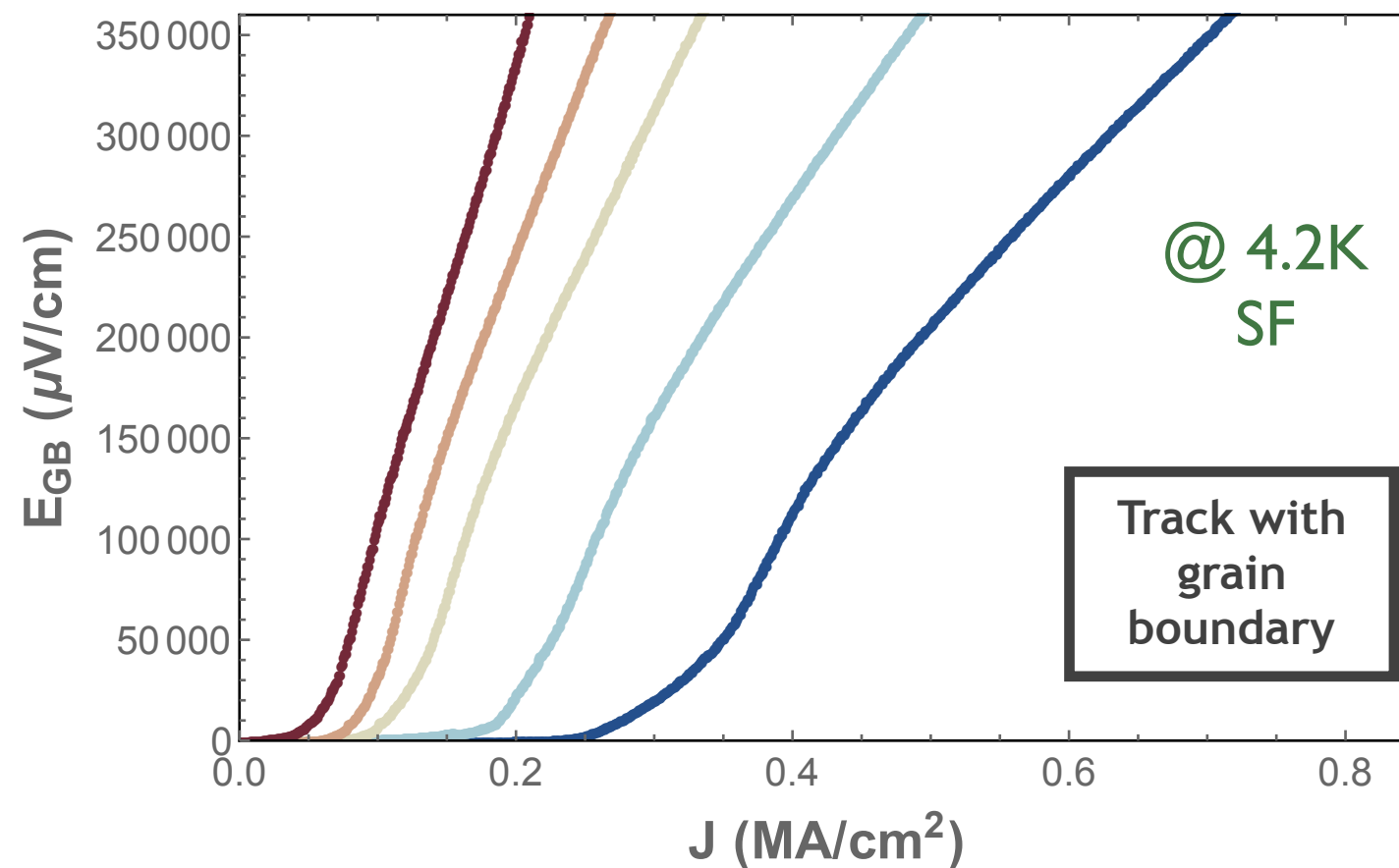


Tuning of a [001] tilt 8° GB



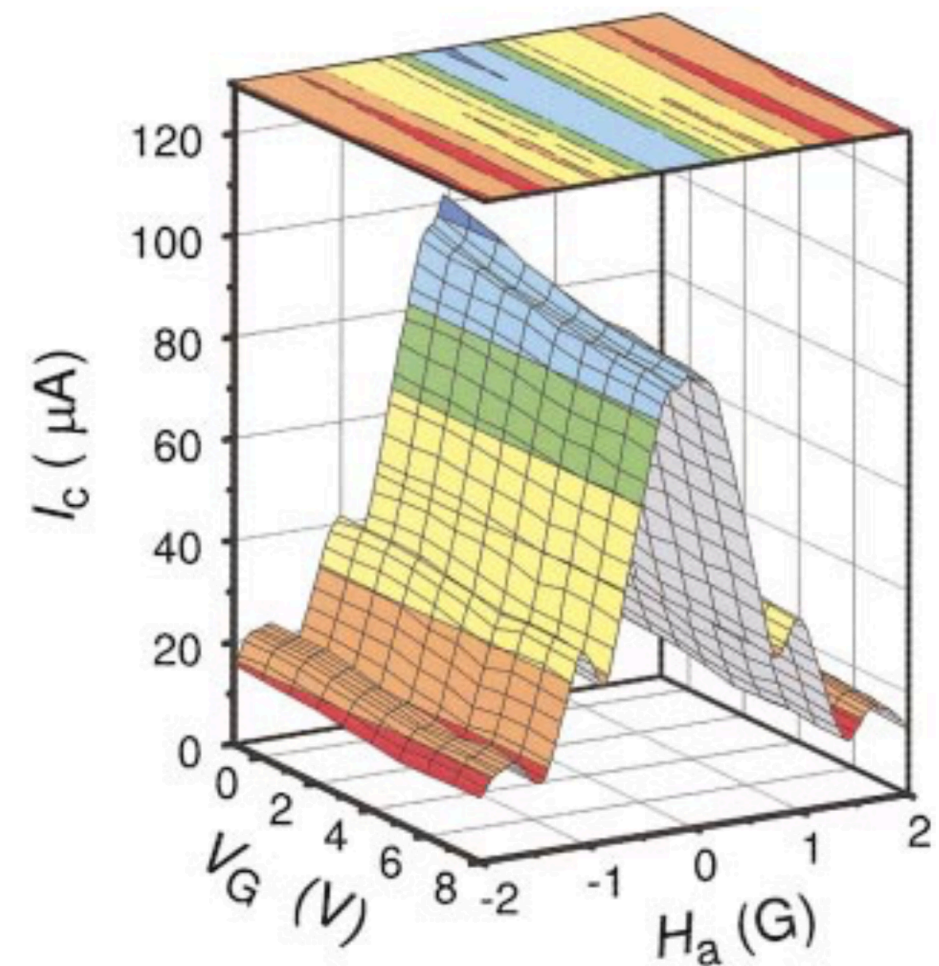
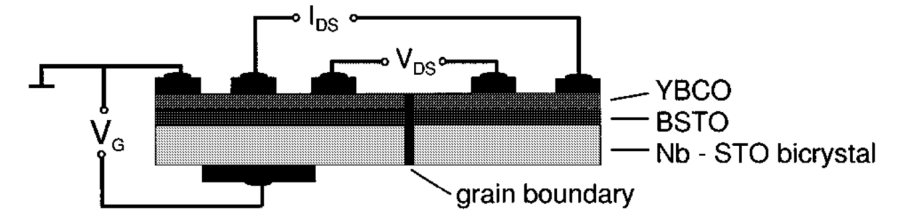
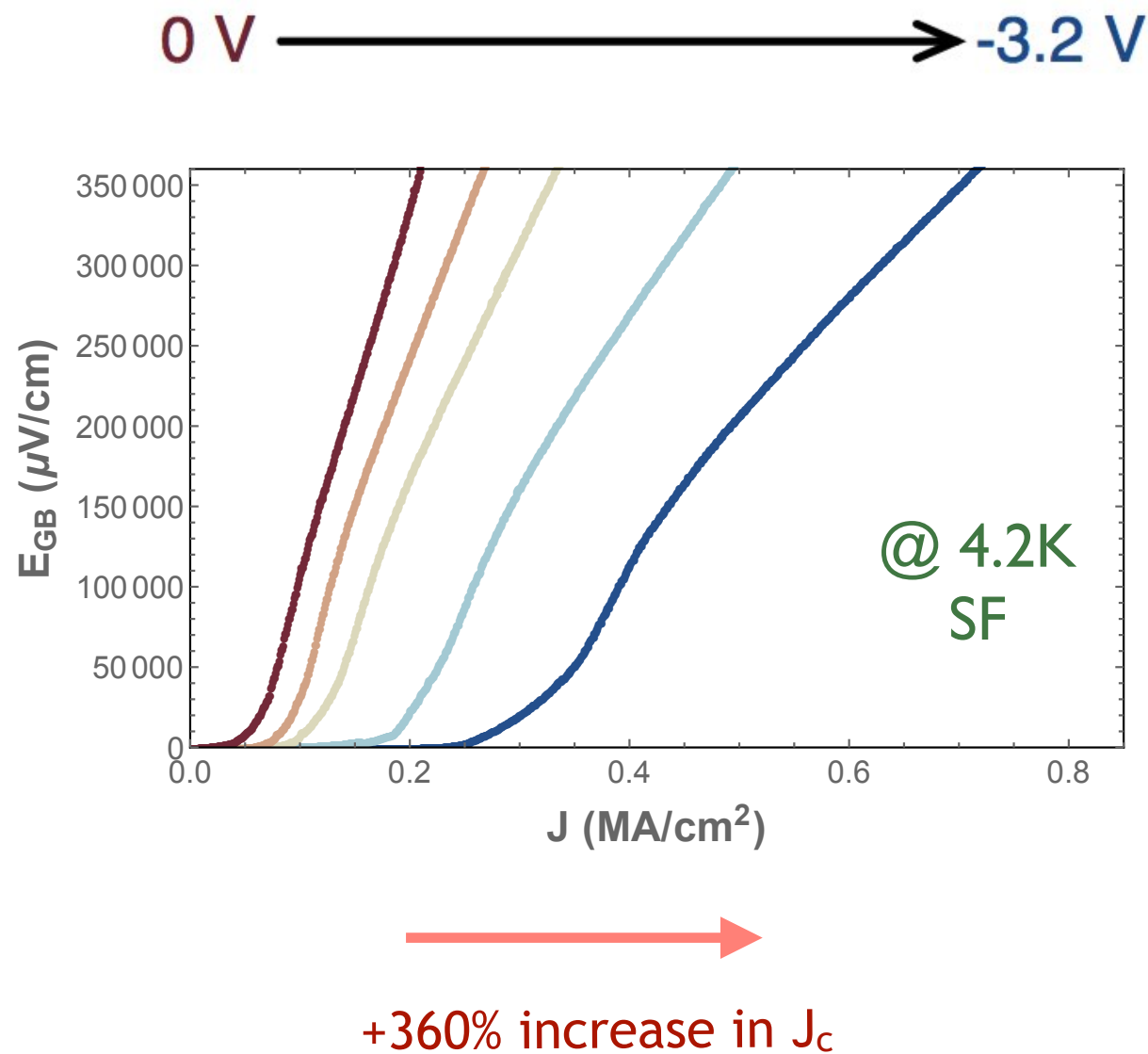
Cooling in remanent field (approx. 7mT)

0 V \longrightarrow -3.2 V



$J_{c,sf}$ is increased by a factor ≈ 5 !

Tuning of a [001] tilt 8° GB



B. Mayer, J. Mannhart, H. Hilgenkamp, APL, 68 3031 (1996)

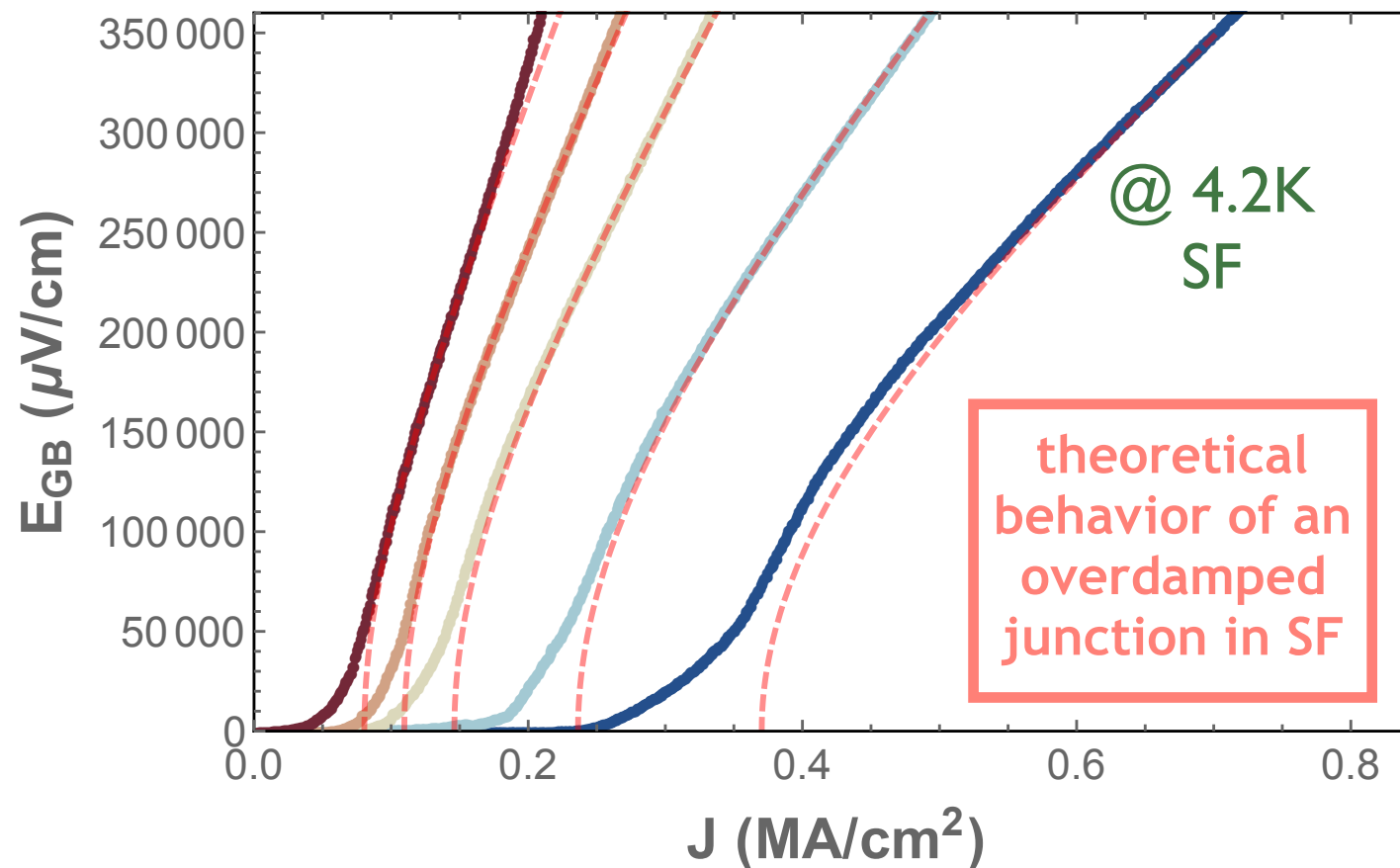
+10%-20% increase in J_c

Tuning of a [001] tilt 8° GB



Cooling in remanent field (approx. 7mT)

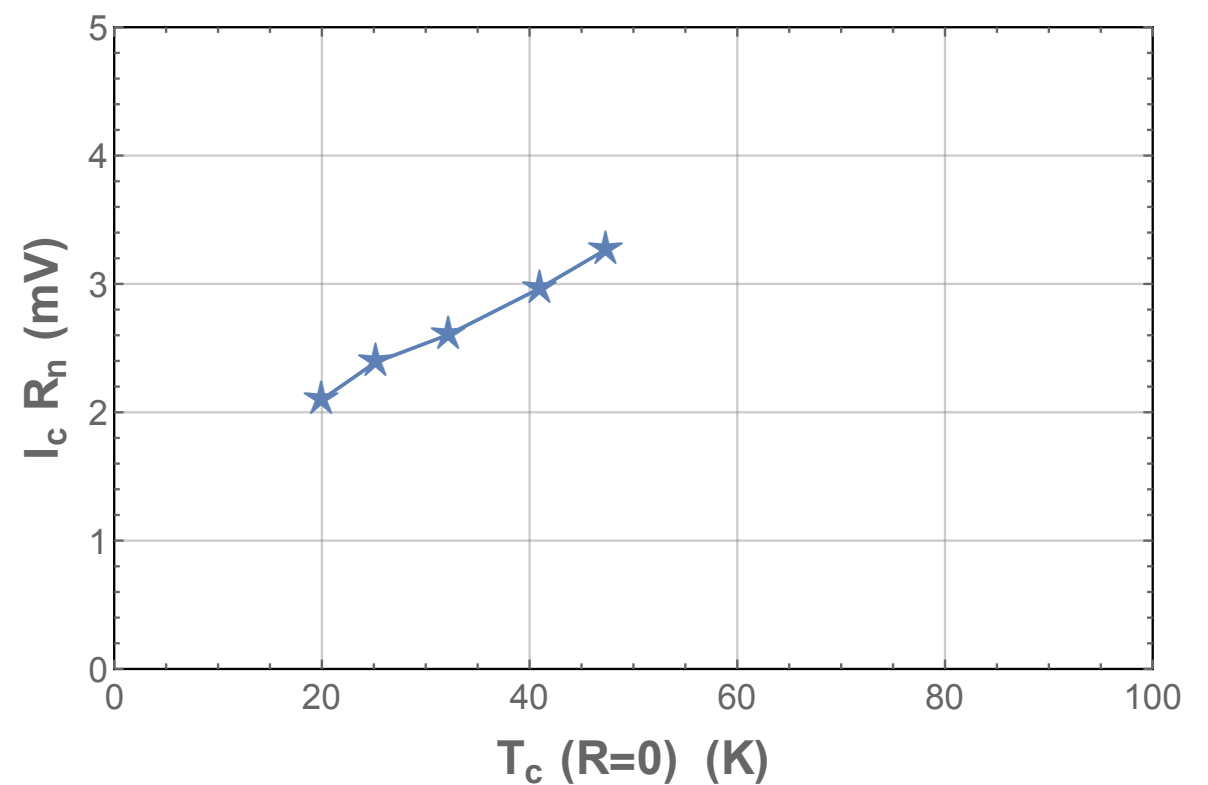
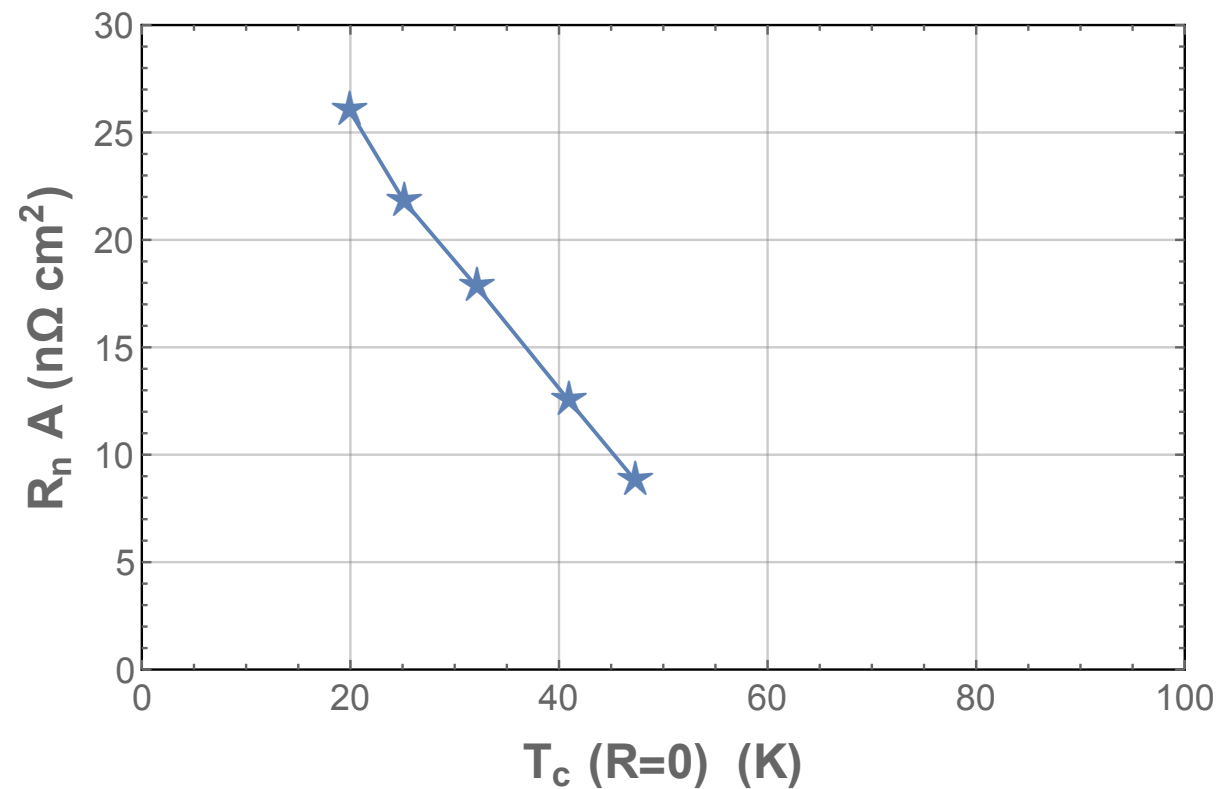
0 V \longrightarrow -3.2 V



Tuning of a [001] tilt 8° GB



Extrapolating our results (not recorded in absolute zero field) within the RCSJ model gives :

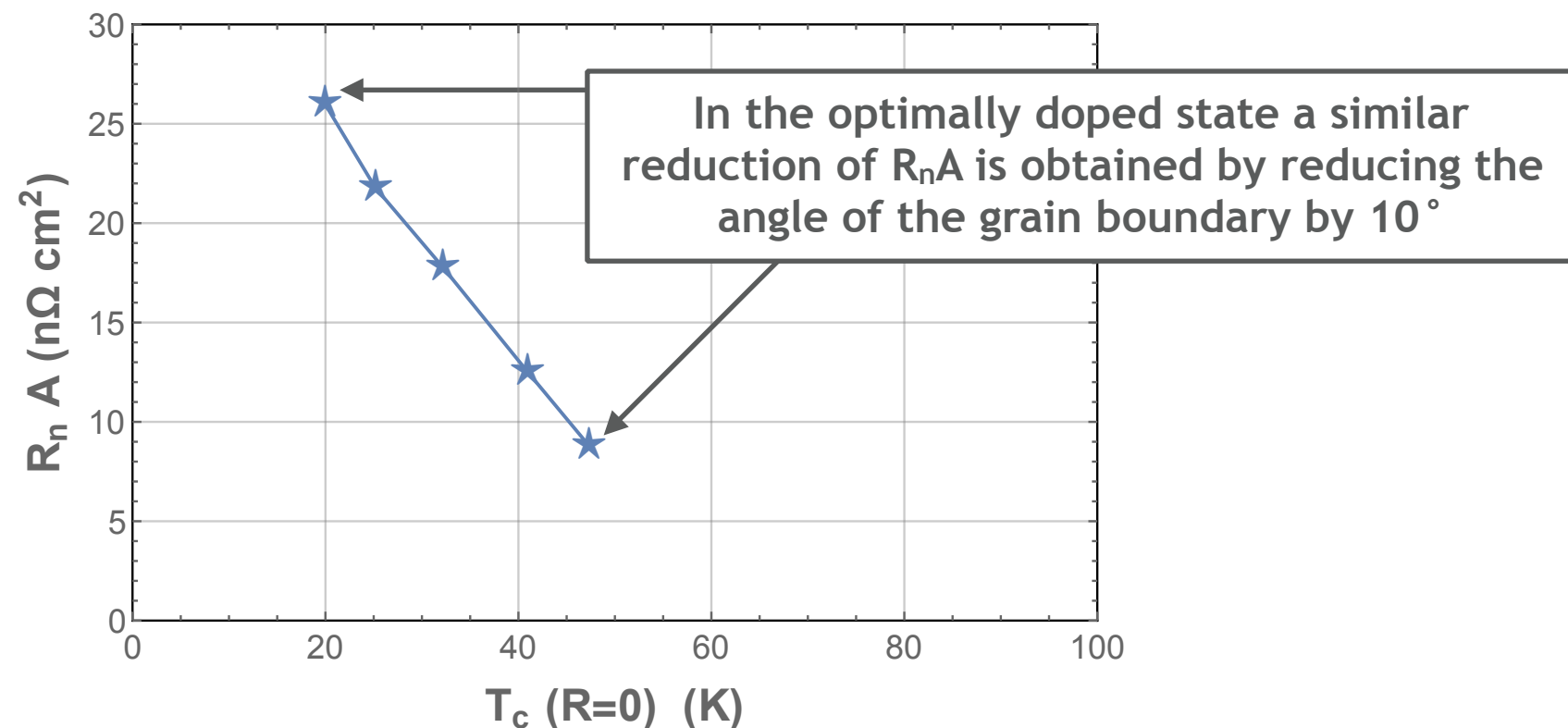


The parameters of the junction are strongly improved

Tuning of a $[001]$ tilt 8° GB



Extrapolating our results (not recorded in absolute zero field) within the RCSJ model gives :

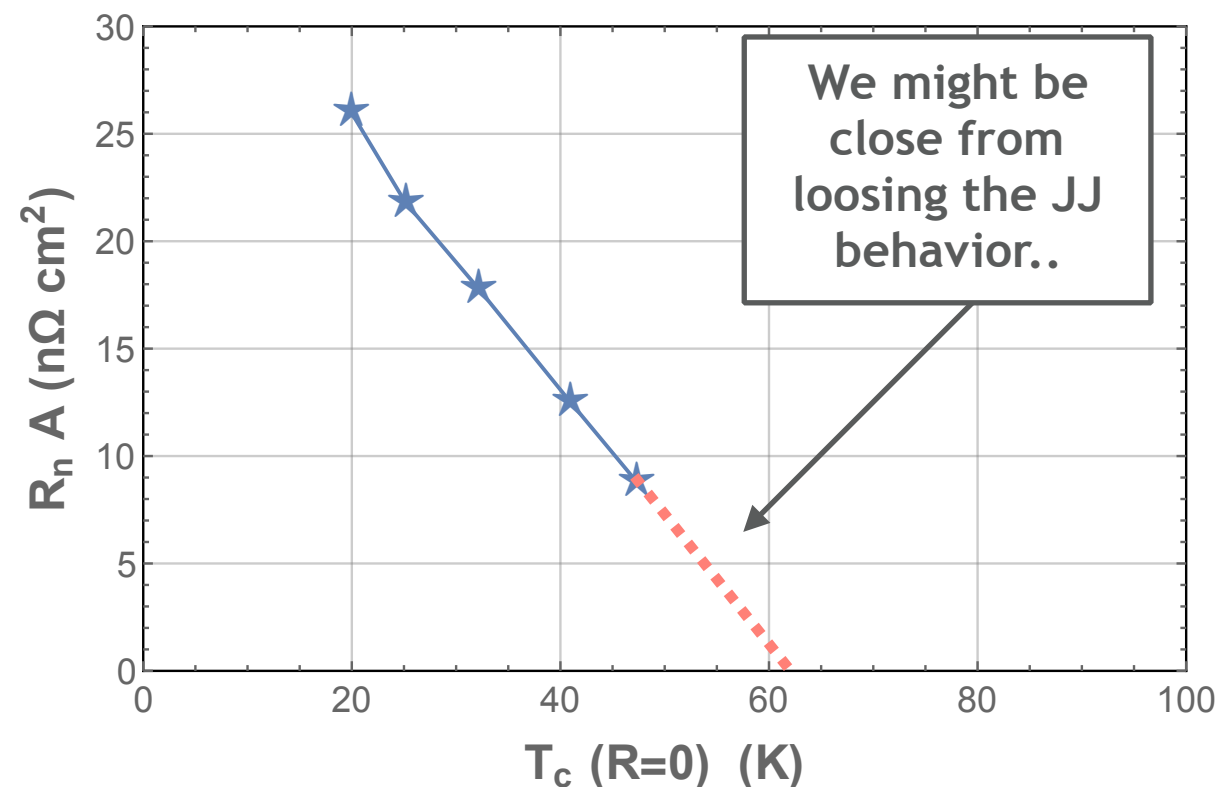


The parameters of the junction are strongly improved

Tuning of a [001] tilt 8° GB



Extrapolating our results (not recorded in absolute zero field) within the RCSJ model gives :

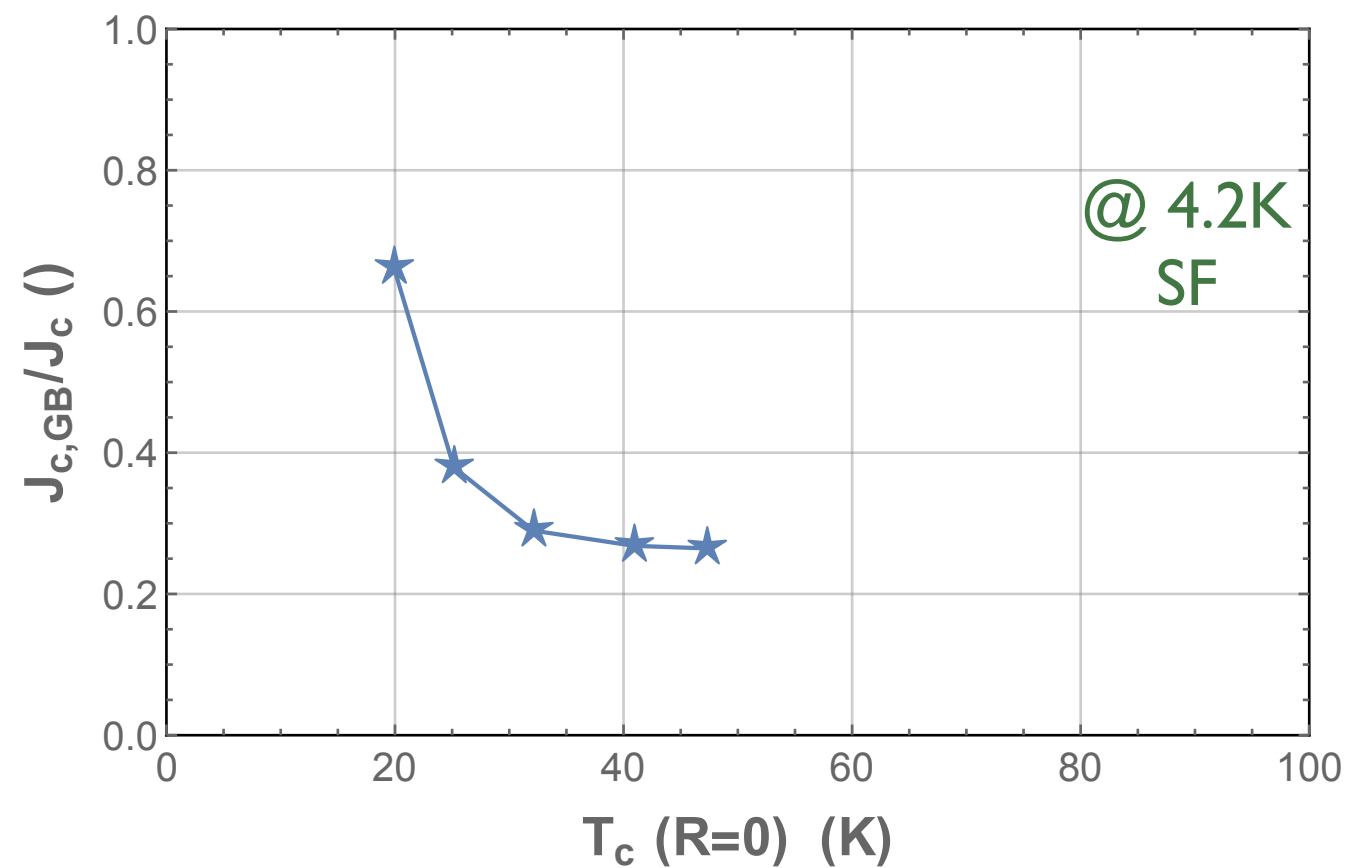


The parameters of the junction are strongly improved

Tuning of a [001] tilt 8° GB



Yet $J_{c,GB}/J_c$ displays a surprising behavior



Tuning of a [001] tilt 8° GB



But $J_{c,GB}$ and J_c have different relation to the superfluid density :
(estimated by $1/\lambda^2$, λ : London penetration depth)

$$J_{c,GB} \propto 1/\lambda^2 \text{ while } J_c \propto (1/\lambda^2)^{3/2}$$

Tunneling of
the SC
condensate

valid for a thin
film
(thickness $< \lambda$)

Talantsev and Tallon
Nat. Comm., **6**, 7820 (2015)

Tuning of a [001] tilt 8° GB



But $J_{c,GB}$ and J_c have different relation to the superfluid density :
(estimated by $1/\lambda^2$, λ : London penetration depth)

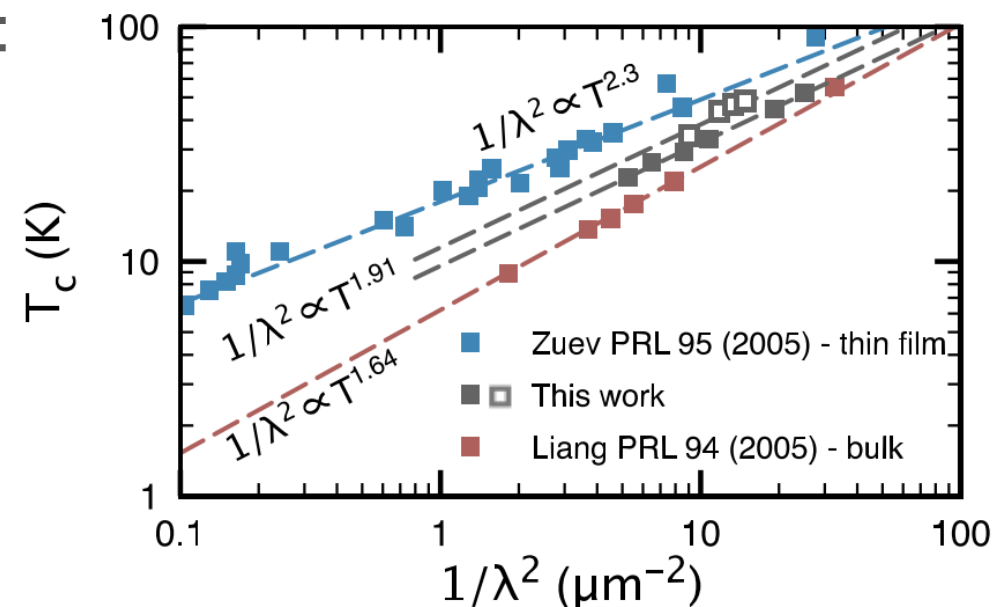
$$J_{c,GB} \propto 1/\lambda^2 \text{ while } J_c \propto (1/\lambda^2)^{3/2}$$

Tunneling of
the SC
condensate

valid for a thin
film
(thickness $< \lambda$)

Talantsev and Tallon
Nat. Comm., **6**, 7820 (2015)

From a previous study :

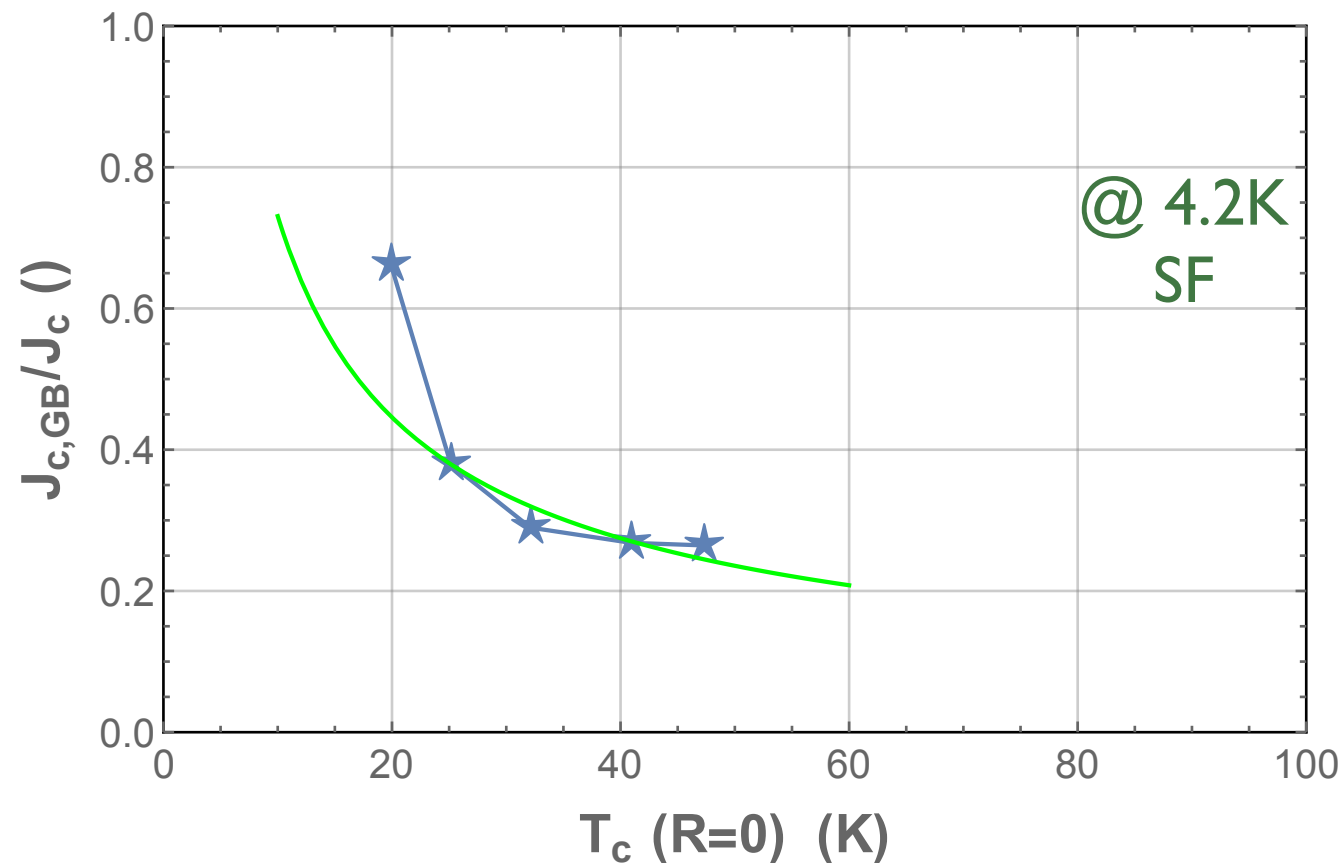


A. Fête, L. Rossi, A. Augieri, C. Senatore, APL **109** 192601 (2016)

Tuning of a [001] tilt 8° GB



Taking into account this yields a relatively good fit



Refinements of this model shall include a dependence of the barrier height with electric field effect and the evolution of the coherence length across the phase diagram

Other angles

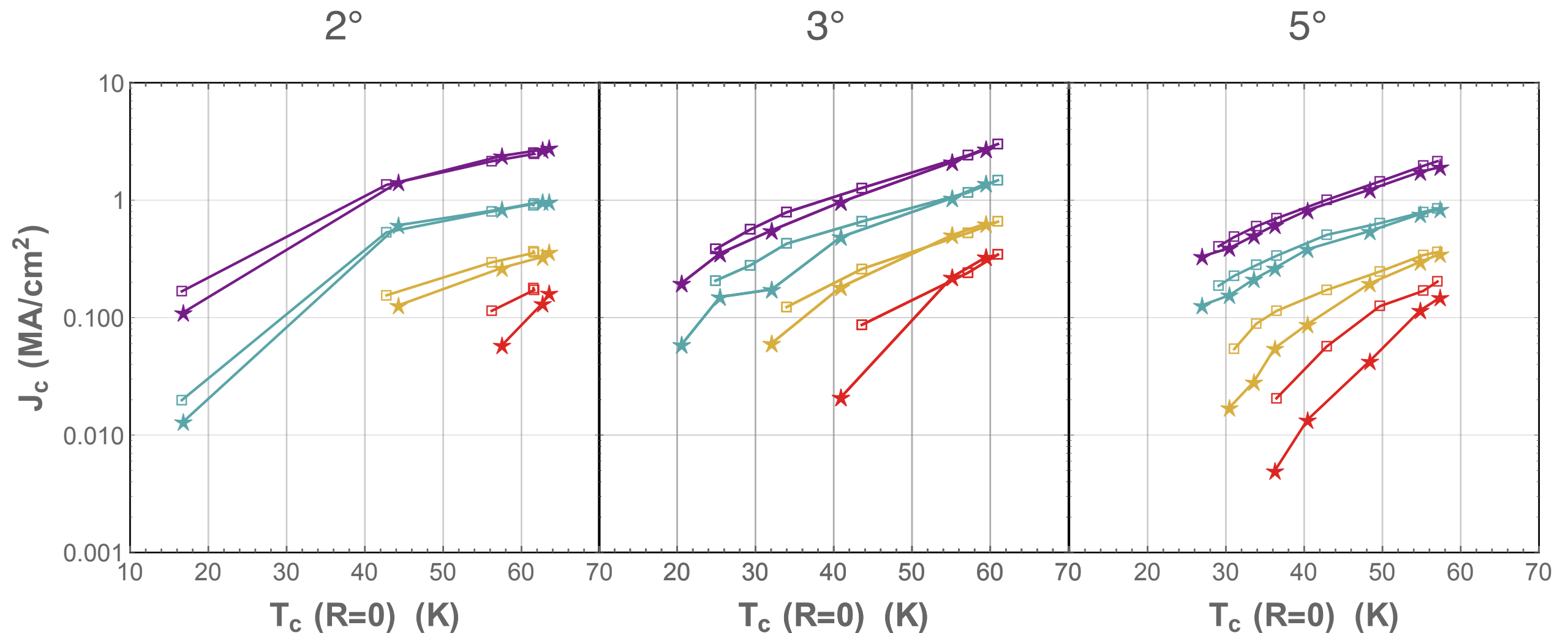


Given the vicinity of the transition from JJ (weak-link) to strong link behavior we explored lower GB angles, namely :

□ reference channel (no GB)

★ channel with GB

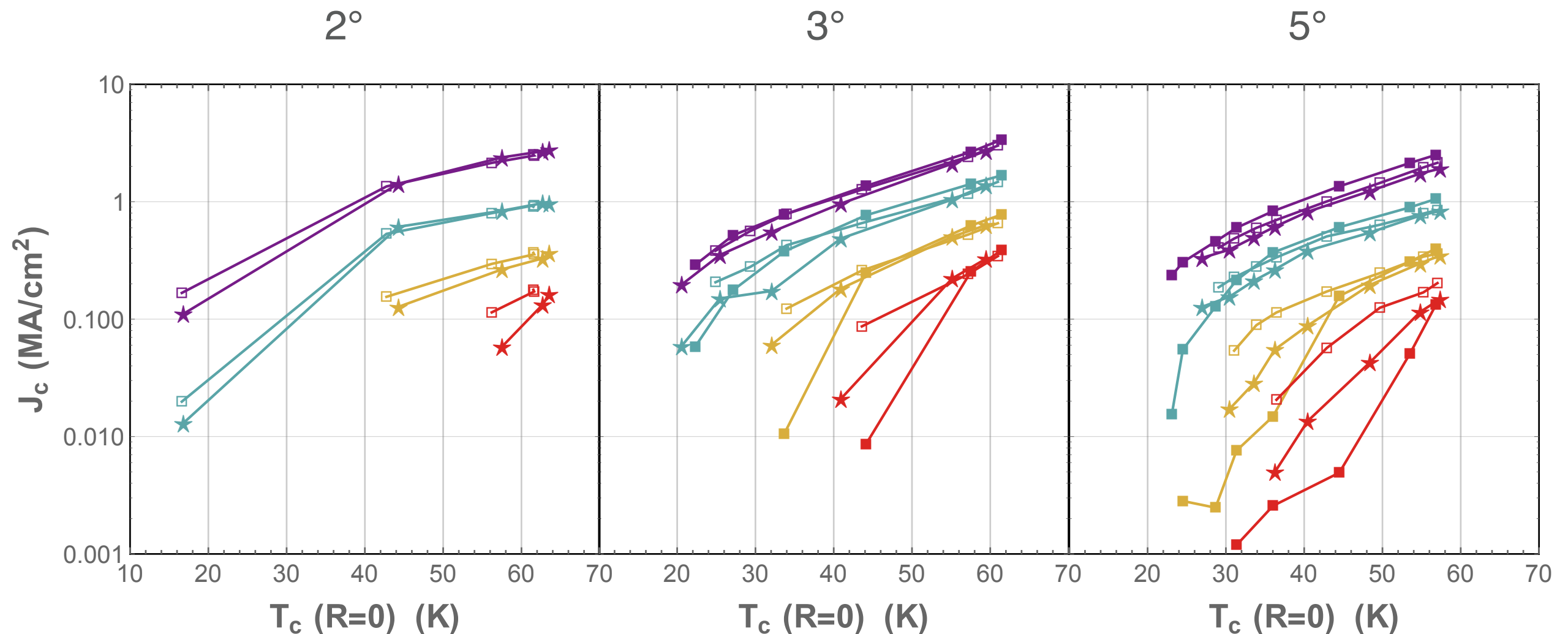
0 2 8 19 (T) @ 4.2K



Other angles



Checking against a second reference channel on the same device makes it much more complicated to be conclusive



Facts :

- 1) A strong tuning of the transport across an 8° grain boundary was achieved.
- 2) For lower angles the transparency of the grain boundaries is such, that the tuning, if present, is hidden by data scattering

Perspectives :

The vicinity of the strong link regime for films grown on 8° bicrystals and the difficulty to observe any difference between inter- and intra-grain transport for films on 2° to 5° bicrystals provide the following research orientation :

- 1) Find 7° bi-crystals and repeat
- 2) Work with thicker films (able to sustain higher initial doping) hoping that the limited penetration depth of the electric field won't be detrimental

**- Thank you for your
attention -**

Alexandre Fête